Pavel Krejčí; Eyram Kwame; Harbir Lamba; Dmitrii Rachinskii; Andrei Zagvozdkin
A continuum of path-dependent equilibrium solutions induced by sticky expectations

Applications of Mathematics, Vol. 68 (2023), No. 6, 751–793

Persistent URL: http://dml.cz/dmlcz/151939

A CONTINUUM OF PATH-DEPENDENT EQUILIBRIUM SOLUTIONS INDUCED BY STICKY EXPECTATIONS

Pavel Krejčí, Praha, Eyram Kwame, Accra, Harbir Lamba, Fairfax,
Dmitrii Rachinskii, Andrei Zagvozdkin, Richardson

Received September 26, 2022. Published online November 6, 2023.

Abstract. We analyze a simple macroeconomic model where rational inflation expectations are replaced by a boundedly rational, and genuinely sticky, response to changes in the actual inflation rate. The stickiness is introduced in a novel way using a mathematical operator that is amenable to rigorous analysis. We prove that, when exogenous noise is absent from the system, the unique equilibrium of the rational expectations model is replaced by an entire line segment of possible equilibria with the one chosen depending, in a deterministic way, upon the previous states of the system. The agents are sufficiently far-removed from the rational expectations paradigm that problems of indeterminacy do not arise.

The response to exogenous noise is far more subtle than in a unique equilibrium model. After sufficiently small shocks the system will indeed revert to the same equilibrium but larger ones will move the system to a different one (at the same model parameters). The path to this new equilibrium may be very long with a highly unpredictable endpoint. At certain model parameters exogenously-triggered runaway inflation can occur.

Finally, we analyze a variant model in which the same form of sticky response is introduced into the interest rate rule instead.

Keywords: macroeconomic model; rational expectation; hysteresis play operator; equilibrium point; path-dependence; sticky inflation

MSC 2020: 37N40, 47J40

1. Introduction

Modern macroeconomics has been dominated by a modeling framework in which the economy is assumed to always be at (or rapidly moving back towards) a unique and stable equilibrium. This has had profound implications both for the way in which the modelers perceive real-world events and their policy prescriptions for dealing with them.

The first author was supported by the GAČR Grant No. 20-14736S.

DOI: 10.21136/AM.2023.0229-22

The critiquing of equilibrium models has a long history which we shall not attempt to detail here. But many antagonists, see for example [32], [19], [34], [10], have eloquently pointed out profound issues concerning the assumed equilibrating processes and the ways in which the 'aggregation problem' was being solved. In this paper we will focus upon one specific pillar of the equilibrium approach which is the assumption of rational expectations introduced by Muth in 1961 [30]. This posits that not only are individuals perfectly rational, optimizing, far-sighted and independent of each other but that their expectations about future uncertainties are in agreement with the model itself.

Our mathematical analysis, and the supporting numerics, rigorously show that, when rational expectations about future inflation are replaced by an aggregated 'sticky' expectation, a simple macroeconomic model changes from a unique equilibrium system to one with an entire continuum of path-dependent equilibria. The form of stickiness that we use is, to our knowledge, new in a macroeconomic setting and differs from, for example, the stickiness of the Calvo pricing model [8], where hypothetical agents are only allowed to adjust (to the correct price) at a fixed rate.

The way in which we incorporate stickiness into the model will be justified and described more fully below but, briefly, our sticky variables can only be in one of two modes. They are either currently 'stuck' at some value or they are being 'dragged' along by some other (related) variable because the maximum allowable difference between them has been reached. Each of these modes (which we shall also refer to as the 'inner' and 'outer' modes, respectively) can be analyzed separately as linear systems using standard stability techniques. However, the full 'hybrid' system is nonlinear and displays far richer dynamics in the presence of exogenous noise and shocks.

It must be emphasized right away that our modelling approach and analytical tools are not restricted to inflation expectations or even to macroeconomics. The form of stickiness described above belongs to a class of operators that have well-understood and very desirable properties. These have already been used to develop nonequilibrium asset-pricing models [24], [25] that have (almost-) analytic solutions.

Here we are able to prove the existence of an entire line interval of feasible equilibrium points, examine their stability, and identify some important consequences of path dependence regarding the effects of exogenous shocks and policy changes upon the state of the system. Furthermore, these changes are realistic in that they both correspond closely to observed, but potentially puzzling, economic situations and are robust enough to be observed numerically in more sophisticated variants of the model.

The level of mathematical knowledge required to follow most of the arguments is not much more than is needed to examine the existence and stability of equilibria in more traditional, fully linear, models. Another useful aspect of this simple model is

that the stickiness can be smoothly 'dialed back' to zero and the unique equilibrium case is recovered. Or, to put it another way, we can rigorously show that a plausible, boundedly rational *yet fully analyzable*, change to a fully rational model significantly alters the qualitative behaviour of the system in recognizable ways.

At the time of writing (the summer of 2023) the world economy has been hit by severe shocks in both supply and demand, caused by the COVID pandemic and the invasion of Ukraine. A rapid rise in inflation has forced Central Banks to respond and there is much debate about how high interest rates will need to rise and whether the initial responses were rapid enough. There has also been much criticism, both internally and externally, of the models used by Central Banks and their inability to forecast inflation sufficiently well—even over the short term. For the first time in decades, some Central Banks appear to be at least as concerned with inflation expectations as the level of inflation due to fears of a runaway wage-price spiral. This makes both the stickiness of those expectations and delays in the effects of Central Bank policy matters of great modeling significance.

Before introducing the model and starting the mathematical analysis, it is worth stepping back to consider the effects of stickiness and friction in physical rather than economic systems. This helps develop our intuition about the nature of equilibria in such systems but the comparison also offers a high-level explanation of the failure of mainstream economics to foresee economic crises, even when not caused by exogenous shocks, and then to formulate consistent policy responses.

1.1. Economics, earthquakes and friction. In early 2009, Alan Greenspan, former Chairman of the Federal reserve, wrote the following:

"We can model the euphoria and the fear stage of the business cycle. Their parameters are quite different. ... we have never successfully modelled the transition from euphoria to fear." —Alan Greenspan, *Financial Times*, March 27th 2009.

The implication is that Central Bank models work well 'most of the time' with suitably calibrated parameters. Occasionally, the parameters suddenly change but once these are measured, the model again works well in the neighbourhood of a new equilibrium.

The above response to models that suddenly fail is only justified when the transitions between euphoria and fear and the changes in parameters are truly exogenously triggered. If they are due to endogenous causes, then the model was never really working before the transition and it probably will not after the transition either!

A useful analogy here is with earthquakes and seismology. Earthquake zones *appear* to be stable (i.e., in an equilibrium) for very long periods of time with only very brief, but violent, 'transitions'. A tectonic-plate-denying 'equilibrium seismologist' might argue that the earthquake-free equilibrium model was essentially correct

except for some occasional unpredictable exogenous events (unobserved meteorite strikes!?) that did not in any way cast doubt on the modelling assumptions.

Of course, earthquakes are almost always endogenously generated and the analogy can be pushed further. An earthquake is a very fast shift from one (meta-)stable[1] internal configuration to another and this leads us consider the concept of 'balance-of-forces' in both physics and economics.

Ever since the time of Walras and Jevons the idea that there should be a complete and unique set of equilibrium prices that exactly balances all of the competing needs and desires of economic agents has offered a compelling view of a perfectly balanced economy with tâtonnement processes somehow achieving this outcome. But this view is based upon a comparison with physical systems that is misleading. A spring or piece of elastic subject to competing forces will achieve a unique equilibrium but this is because there is no complex internal structure capable of absorbing any of the stresses without yielding.

A more complicated physical system such as a tectonic fault line has myriad internal configurations capable of balancing the forces applied to it—up to a point. Which particular configuration exists at any given moment will depend upon the previous states of the system. And when one small part of the fault line suddenly shifts, this can transfer excess stress to neighbouring parts resulting in a large cascading failure/earthquake. There is a balance of forces before the earthquake and after the earthquake but not *during* the earthquake!

A modern economy is arguably the most complicated man-made construct on the planet with an immensely intricate internal description which cannot simply be averaged away. The analogy is also useful in that the fundamental source of earthquakes is friction. Without it, continental plates would gracefully and safely glide rather than stick and then briefly grind. Frictions and stickiness are present in many forms in an economy or financial system and it should not be a surprise if they cause similar qualitative effects.

This brings us to the notion of timescales. In an equilibrium system there is no notion of *any* timescale except for ones imposed exogenously[2]. If one examines an earthquake fault line on a long-enough timescale, maybe tens of thousands of years, then it does not look like an equilibrium at all. The mere presence of frictional effects can introduce surprisingly long timescales into a system via the existence of metastable states.

[1] Metastability in physics is when a system can stay in a particular state for an indefinite amount of time even though it is not the state of lowest energy. It occurs when there is some kind of barrier to true equilibration.

[2] There is no notion of history either. If a system is at its unique equilibrium, there is no way of telling where it has been.

If economies feel like they are close to a unique equilibrium, maybe that's because most of the time tomorrow does indeed turn out to be a lot like yesterday! Over short timescales, unique equilibrium models will frequently appear to be working—especially when their parameters are being updated to match incoming real-world data!

Finally, it must be pointed out that the analogy between earthquakes and the models that we will analyze below is not perfect. Fault lines are being consistently forced in a single direction while the changes experienced by economies are more random. Also, our main model has a very small number of variables and only one sticky component and so 'slippage cascades' are not possible. However, even a single sticky component allows for the existence of an entire interval of equilibria and complicated transitions between them.

1.2. Permanence and path-dependence. If the presence of stickiness/frictions in economics does indeed induce a myriad of coexisting equilibria, then phenomena that are not possible (or require a posteriori model adjustments) in unique equilibrium models become not just feasible but inevitable. Perhaps the most obvious of these is *permanence*, also known as remanence, where a system does not revert to its previous state after an exogenous shock is removed. It is of course a central concern of macreconomics whether or not economies affected by, say, significant negative shocks can be expected to have permanently reduced productivity levels.

For the models studied in this paper, sufficiently small shocks (whether exogenous or applied by policy makers) will not change the equilibrium point and a standard linear stability analysis determines the rate at which the system returns to it. Larger shocks will move the equilibrium point along a line of potential equilibria in the expected direction. But even larger shocks may move the system far enough away from the equilibrium interval that the return path and ending point on the interval are very hard to predict. Furthermore, in neither of the last two cases will the system exhibit a tendency to return to its pre-shocked state—the model displays true permanence. And the model parameters alone cannot determine which equilibrium a system is currently in without knowing important information about the prior states of the system—true path dependence. This does not, however, prevent the system from being iterated once the initial conditions are *fully* specified.

1.3. Sticky models and indeterminacy. The most widely-used sticky models are the sticky-prices of Calvo [8] and the sticky-information of Mankiw and Reis [28]. These models are conceptually very similar to each other in that agents do not instantaneously move to the 'correct' price or opinion but rather do so at a fixed

rate and can be represented mathematically by introducing a delay term into the relevant equations. In the absence of noise the same optimal equilibrium solution will be reached as if the stickiness were absent.

Continua of possible equilibria can also occur in such models (see for example [4], [13]) and is considered an extreme form of *indeterminacy*. This is especially problematic within a rational expectations framework since it makes it (even) harder to justify how the agents' expectations can be consistent with the model.

Our hypothetical agents are less rational than those above. They are truly stuck (not just delayed) until forced to adjust by the discrepancy with the actual inflation rate.[3] If an equilibrium is reached, it is chosen by the prior states of the system and not by modeling assumptions about the future and, as we shall see, a continuum of equilibria is an intrinsic feature and not an inconvenience that occurs only in certain special cases (such as a passive interest-rate policy [8], [2]).

The research into how expectations are formed is extensive but far from conclusive, see for example [11], [33], [6], [9], [29]. However, the idea of threshold effects and a 'harmless interval' of inflation is not new in economics [5], [26], [35], [14], [20]. In the absence of any exogenous forcing it would be very easy to distinguish between Calvo-type stickiness and the stuck-then-dragged behavior we investigate here—indeed, Calvo stickiness would most likely be observed since agents could tell far more easily over time that, for example, their wage demands were too low and they were losing purchasing power. However, given the uncertainty of reality and the very limited cognitive skills or interest in forecasting of most economic agents, that may no longer hold.

Our model of expectation formation is thus both mathematically tractable and has some basis in both observed data (see also [15], [16]) and models of bounded rationality. As such it provides a potentially useful, analytically tractable, alternative to staggered/delayed models—and one with additional complexity and explanatory power.

1.4. Bounded rationality and aggregation. As mentioned above, the standard approach to the problem of aggregating expectations is to introduce a 'Representative Agent' whose expectations are fully-informed and rational and consistent with the model itself. Here, an aggregation of *boundedly* rational agents into a similar Representative will be required.

A similar problem was encountered in De Grauwe [12]. In [12] both the expectations terms in inflation and output gap were linear combinations of the expectations of two kinds of agent—rational 'fundamentalists' and boundedly rational

[3] This is now very close to the situation where a frictional force has to be overcome before an object will move.

'extrapolators'—with the probability of an agent using each being dictated by discrete choice theory [1], [7]. In other words, discrete choice theory was the aggregating mechanism used to avoid ending up with an agent-based model where each agent had to be individually simulated. It was then shown numerically that cycles of booms-and-busts occurred with changes in the 'animal spirits' and corresponding nonGaussian 'fat-tailed' distributions for the model variables.

We start from the empirical evidence cited above that individual agents' expectations are often sticky and may lag behind the currently observable values before they start to move. We also posit that this gap between future expectations and current reality cannot grow too large. This leads us in a very natural way to the play operator that is described fully in Section 2.1 as a model for each individual agent's expectations. However, the composition/aggregate of even two play operators is no longer a play operator – although the output will still display inactive (as well as less active) modes and there is still a maximum allowable difference between the input and output.

Play operators and their complements, stop operators, are special cases of a wider class of Prandtl-Ishlinskii or PI operators that have a remarkable aggregation property. When connected together in an arbitrary network (under mild technical conditions), they collectively act as a single, but different, PI operator. Thus, as long as individual agents are represented by PI operators, there is a rigorous aggregation process by which a network of interacting heterogeneous agents can be reduced to a single representative agent. This ability to rigorously aggregate nontrivial agents is very unusual – and not just within economics. Furthermore, this new composite PI operator can be identified analytically in simple cases or, more generally, by measuring the network's response to a monotonic input. The result and further references to PI operators can be found in [23].

Returning to the expectations aggregation problem, we can imagine agents in the economy/model being connected in a way that reflects how much influence each agent's expectations affects their neighbors on the network. Then each agent's individual inflation expectation can be modeled by a play operator (or by something 'close' within the space of PI operators) whose input is some combination of both the actual inflation rate and the expectations of their neighbors. By the composition property of PI operators, the aggregate response will also be a (more complicated) PI operator that should nevertheless still have stuck, less active, and more active regimes while still limiting the difference between the actual and aggregated expected inflation.

Importantly, when agents are connected via a network, internal 'cascades' of changes in expectations can occur, bringing us closer to the previous earthquake analogy. For example, if one especially significant agent suddenly starts to increase their

expectation of inflation, this may trigger increases in its network neighbors' expectations and so on. Nevertheless, such cascades can still be completely represented by a single composite PI operator. If cascades can occur, then the output of the operator when given a smoothly varying input will have corresponding discontinuities [23].

Rather than study a sticky expectations model with a single, complicated, aggregated PI operator, we shall instead assume that the aggregated PI operator is itself just a single play operator. This case can be analyzed in detail and is a necessary prerequisite for a deeper understanding of the dynamics of such systems (although we do also present simulations for a multi-agent model in Section 3.7). Also, the space of all possible boundedly rational perturbations to rational models is very large and very hard to study rigorously or even define. This makes the existence of an analytically tractable, plausible, boundedly-rational variant of a rational model, a subject of independent interest, and provides an additional justification for our nonstandard but conceptually simple Representative Agent.

1.5. Outline of the paper. We start from a dynamic stochastic general equilibrium (DSGE) macroeconomics model, which includes aggregate demand and aggregate supply equations

$$y_t = y_{t-1} - a(r_t - p_t) + \varepsilon_t, \quad x_t = b_1 p_t + (1 - b_1)x_{t-1} + b_2 y_t + \eta_t \tag{1}$$

augmented with the rate-setting rule

$$r_t = c_1 x_t + c_2 y_t, \tag{2}$$

where y_t is output gap (or unemployment rate, or another measure of economic activity such as gross domestic product), x_t is inflation rate, r_t is interest rate, p_t is the economic agents' aggregate expectation of future inflation rate and ε_t, η_t are exogenous noise terms. All the parameters are nonnegative and in addition, $b_1 < 1$. This model is close to the starting model used in [12] but simpler in that we do not include the aggregate expectation of the output gap and the correlation between the subsequent values of the interest rate. We also choose to remove the noise term from the interest rate update rule. The inclusion of such factors does not affect our most significant qualitative observations, but would complicate some aspects of the rigorous analysis that we present.

The novelty of our modeling strategy is in how we define the relationship between the aggregate expectation of inflation p_t and the inflation rate x_t. This relationship is defined precisely in the next section where we introduce the play operator to model the economic agents' aggregate expectation of future inflation.

In Sections 2.4–2.5 we present the main stability analysis for various parameter regimes, with some details relegated to Appendices. The stability properties of the

system are not as clear cut as in a truly linear system. In fact, our equations define a *piecewise linear* (PWL) system, and certain nonlinear effects come into play. In particular, in nonlinear systems an equilibrium may only be *locally* stable. This means that the equilibrium is only stable to perturbations of a certain size—ones that do not move the system outside of a 'basin of attraction'—and this phenomenon is responsible for much of the interesting dynamics in the presence of shocks.

In Sections 3.1–3.6 we present various numerical simulations. We are particularly interested in the transitions between equilibrium states caused by exogenous shocks, and the effects of increasing or decreasing stickiness. Where possible we compare results against the nonsticky model. Permanence is the rule, not the exception and there are even parameter regimes where a large enough shock will completely destabilise an apparently stable system via a runaway inflation mechanism.

We also compare the statistical output of the model against that of De Grauwe [12] at similar parameters and see the same boom-and-bust cyclicality and heavy-tailed distributions.

Then, in Section 3.7 we briefly consider a more complicated version of the model with three representative agents all with different levels of stickiness. This is primarily to demonstrate that multiple play operators can indeed be used together to simulate different representative agents within a model and that the most important qualitative features are unchanged.

Finally, in Section 3.8 we emphasize that play operators are not just a potential tool for modeling expectations—we remove the stickiness from the inflation expectations and add it into the response of the Central Bank instead. We perform a second stability analysis and obtain some interesting new effects—there is the possibility of (quasi)-periodic behavior in the absence of noise and the stickiness does appear to destabilize equilibria. We conclude with a summary of the main results and some suggestions for future work.

2. The model

2.1. Play and stop operators. We assume the following rules that define the variations of the expectation of future inflation rate p_t with the actual inflation rate x_t at integer times t:

(i) The value of the difference $|p_t - x_t|$ never exceeds a certain bound ϱ;

(ii) As long as the above restriction is satisfied, the expectation does not change, i.e., $|x_t - p_{t-1}| \leqslant \varrho$ implies $p_t = p_{t-1}$;

(iii) If the expectation has to change, it makes the minimal increment consistent with constraint (i).

Rule (ii) introduces stickiness in the dependence of p_t on x_t, while (i) states that the expected inflation rate cannot deviate from the actual rate more than prescribed by a threshold value ϱ. Hence p_t follows x_t reasonably closely but on the other hand is conservative because it remains indifferent to variations of x_t limited to a (moving) window $p - \varrho \leqslant x \leqslant p + \varrho$. The last rule (iii) enforces continuity of the relationship between p_t and x_t and, in this sense, can be considered as a technical modeling assumption that is mathematically convenient.

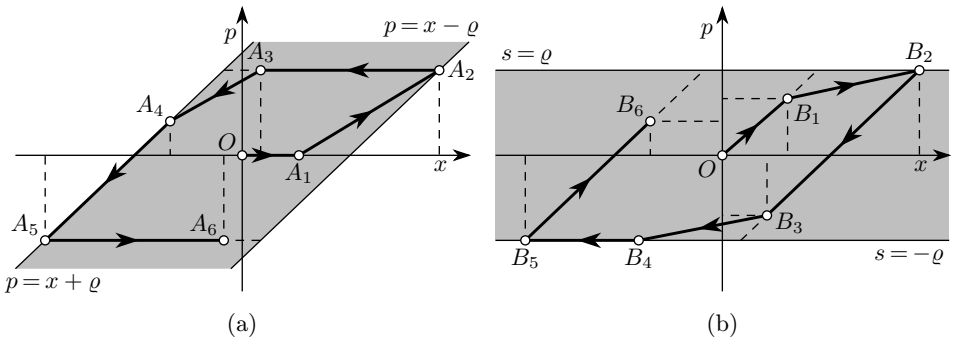

Figure 1. (a) An illustration of the input-output sequence of the (a) play operator and (b) stop operator. (a) The polyline $OA_1A_2A_3A_4A_5A_6$ represents a sample input-output trajectory for the play operator. The input-output pair (x, p) is bounded to the gray strip between the two parallel lines $p = x \pm \varrho$. In [16], this strip is called *band of inactivity*, the line $x = x - \varrho$ is called *upward spurt* line while the line $p = x + \varrho$ is called *downward spurt* line. The ouptut p remains unchanged for a transition from (x_{t-1}, p_{t-1}) to the next point (x_t, p_t) as long as the pair (x_t, p_{t-1}) fits to the band of inactivity (for example, the transitions from $A_2 = (x_2, p_2)$ to $A_3 = (x_3, p_3)$ with $p_2 = p_3$ or from $A_5 = (x_5, p_5)$ to $A_6 = (x_6, p_6)$ with $p_5 = p_6$). If $x_t > x_{t-1}$ and the point (x_t, p_{t-1}) lies to the right of the inactivity band, then the output increases resulting in the point (x_t, p_t) to lie on the upward spurt curve (for example, the transition from $A_1 = (x_1, p_1)$ to $A_2 = (x_2, p_2)$). Similarly, if $x_t < x_{t-1}$ and the point (x_t, p_{t-1}) lies to the left of the inactivity band, then the output decreases and the point (x_t, p_t) lies on the downward spurt line (for example, the transition from $A_3 = (x_3, p_3)$ to $A_4 = (x_4, p_4)$). (b) The input-output trajectory of the dual stop operator corresponding to the trajectory of the play operator shown in panel (a). Here $s_t = x_t - p_t$; the trajectory is limited to the horizontal strip $-\varrho \leqslant s \leqslant \varrho$ at all times.

Rules (i)–(iii) are expressed by the formula

$$p_t = x_t + \Phi_\varrho(p_{t-1} - x_t) \tag{3}$$

with the piecewise linear saturation function

$$\Phi_\varrho(x) = \begin{cases} \varrho & \text{if } x \geqslant \varrho, \\ x & \text{if } -\varrho < x < \varrho, \\ -\varrho & \text{if } x \leqslant -\varrho. \end{cases} \tag{4}$$

Relationship (3) is known as the *play* operator with *threshold* ϱ, see Fig. 1 (a). A dual relationship

$$s_t = \Phi_\varrho(x_t - x_{t-1} + s_{t-1}) \tag{5}$$

between x_t and the variable

$$s_t = x_t - p_t$$

is referred to as the *stop* operator, see Fig. 1 (b). In the context of our model, s_t measures the difference between the inflation rate and the expectation of the future inflation rate, hence s_t remains within the bound $|s_t| \leqslant \varrho$ at all times. Interestingly, the explicit relationship (3) has been observed in actual economic data [15], [16].

One can think of the play operator as having two modes. A 'stuck mode' where it will not respond to small changes in the input and a 'dragged mode' where the absolute difference between the input and output are at the maximum allowable and changes to the input, in the correct direction, will drag the output along with it. Equations (3) and (7) will now be denoted by

$$p_t = \mathscr{P}_\varrho[x_t], \quad s_t = x_t - p_t = \mathscr{S}_\varrho[x_t], \tag{6}$$

where $\mathscr{P}_\varrho$ and $\mathscr{S}_\varrho$ are the *play* and *stop* operators with threshold ϱ, respectively.

R e m a r k 1. The form (7) of the function Φ_ϱ postulates the same magnitude of response by the representative agent to positive and negative increments of x. However, there is almost certainly an assymmetry in the perception gap such as, for example, in Kahneman and Tversky's behavioral prospect theory [18]. One way to incorporate such an asymmetry in the relationship between the inflation rate x and the expectation p of future inflation rate by the agents, is to adapt rules (i)–(iii) and replace function (4) with the function

$$\Phi_{\varrho_l,\varrho_r}(x) = \begin{cases} \varrho_l & \text{if } x \geqslant \varrho_l, \\ x & \text{if } -\varrho_r < x < \varrho_l, \\ -\varrho_r & \text{if } x \leqslant -\varrho_r, \end{cases} \tag{7}$$

which has different positive thresholds ϱ_l and ϱ_r; formula (3) changes accordingly to

$$p_t = x_t + \Phi_{\varrho_l,\varrho_r}(p_{t-1} - x_t). \tag{8}$$

For example, if $\varrho_l > \varrho_r$, then the agents are responsive to smaller positive increments of the inflation rate compared to its negative increments. By inspection, system (1),

(2), (7), (8) with asymmetric response can be reduced to system (1)–(4) with symmetric thresholds $\varrho = (\varrho_l + \varrho_r)/2$ by the following shift of the variables:

$$y = \widehat{y} - \frac{b_1\delta}{b_2}, \quad x = \widehat{x} + \varkappa\delta, \quad p = \widehat{p} + (1+\varkappa)\delta,$$

where

$$\delta = \frac{\varrho_l - \varrho_r}{2}, \quad \varkappa = \frac{b_1c_2 + b_2}{(c_1-1)b_2}.$$

Keeping in mind this simple transformation, we restrict our further analysis to system (1)–(4).

R e m a r k 2. Without loss of generality, one can set the threshold ϱ of the play operator to unity. Indeed, the simple rescaling of the variables and noises, which replaces y, p, x, r, ε, η with ϱy, ϱp, ϱx, ϱr, $\varrho\varepsilon$, $\varrho\eta$, respectively, preserves linear equations (1), (2), while transforming equation (3) to

$$p_t = x_t + \Phi_1(p_{t-1} - x_t)$$

due to the identity $\Phi_\varrho(\varrho x) = \varrho\Phi_1(x)$. As such, dynamics is controlled by the ratio of the noise amplitude and the threshold, while the threshold ϱ controls the scale of the dynamics.

2.2. A model with sticky inflation expectations. Equations (1) and (2), completed with formulas (3) and (4), form a closed model for the evolution of the aggregated variables x_t, y_t, r_t, p_t. However, the dependence of these quantities at time t upon their values at time $t-1$ is implicit. In order to implement the model, we proceed by solving equations (1)–(4) with respect to the variables x_t, y_t. As shown in Appendix A, the model can be written in the following equivalent form:

$$z_t = Az_{t-1} + s_t d + N\xi_t, \tag{9}$$

where $z_t = (y_t, x_t)^\top$, $\xi_t = (\varepsilon_t, \eta_t)^\top$, the superscript $^\top$ denotes transposition, the matrices A, N and the column vector d are defined by

$$A = \frac{1}{\Delta}\begin{pmatrix} 1-b_1 & a(1-b_1)(1-c_1) \\ b_2 & (1-b_1)(1+ac_2) \end{pmatrix}, \quad N = \frac{1}{\Delta}\begin{pmatrix} 1-b_1 & a(1-c_1) \\ b_2 & 1+ac_2 \end{pmatrix}, \tag{10}$$

$$d = \frac{1}{\Delta}\begin{pmatrix} a(b_1c_1 - 1) \\ -(ab_2 + b_1(1+ac_2)) \end{pmatrix}$$

with

$$\Delta = (1-b_1)(1+ac_2) + ab_2(c_1-1) \tag{11}$$

and $s_t = x_t - p_t$ is defined by the equation

$$s_t = \frac{1}{1+\alpha}\Phi_{\varrho(1+\alpha)}\Big(\frac{b_2}{\beta}y_{t-1} + \frac{(1-c_1)ab_2}{\beta}x_{t-1} + \alpha s_{t-1} + \frac{b_2}{\beta}\varepsilon_t + \frac{1+ac_2}{\beta}\eta_t\Big) \tag{12}$$

with

$$\alpha = \frac{\Delta}{b_1(1+ac_2)+ab_2}, \quad \beta = b_1(1+ac_2)+ab_2. \tag{13}$$

Equations (9), (12) express y_t, x_t and $s_t = x_t - p_t$ explicitly in terms of the previous values of the same variables and the exogenous noises ε_t, η_t. We use these equations in all the simulations that follow.

We shall refer to the variable $s_t = x_t - p_t$ as the *perception gap*. Note that (12) can be equivalently written as (see Appendix A)

$$s_t = \frac{1}{1+\alpha}\Phi_{(1+\alpha)\varrho}(f_t - f_{t-1} + (1+\alpha)s_{t-1}), \tag{14}$$

where

$$f_t = \frac{1}{\beta}(b_2 y_{t-1} + (1-b_1)(1+ac_2)x_{t-1} + b_2\varepsilon_t + (1+ac_2)\eta_t). \tag{15}$$

These formulas define the stop operator with input f_t and threshold $(1+\alpha)\varrho$, which is different from ϱ (cf. (4)). That is, (14) can be written as

$$s_t = \frac{1}{1+\alpha}\mathscr{S}_{(1+\alpha)\varrho}[f_t]$$

using the notation (6). It is important to note that the transition from system (1)–(4) to equations (9), (12) (equivalent to (9), (14), (15)) is justified under the condition that α is positive, and we assume this constraint to hold in the rest of the paper. In particular, $\alpha > 0$ whenever $c_1 > 1$ (see Section 2.5).

2.3. An entire line segment of equilibrium points. We begin the analysis of the model (9), (12) by looking at the case of no exogenous noise, i.e., we set $\xi_t = 0$ and consider the equations

$$z_t = Az_{t-1} + s_t d, \quad z_t = (y_t, x_t)^\top, \tag{16}$$

$$s_t = \frac{1}{1+\alpha}\Phi_{\varrho(1+\alpha)}\Big(\frac{b_2}{\beta}y_{t-1} + \frac{(1-c_1)ab_2}{\beta}x_{t-1} + \alpha s_{t-1}\Big) \tag{17}$$

instead of (9) and (12). This model has an entire line segment of equilibrium points which corresponds to a continuum of feasible equilibrium states of the economy as

a function of the inflation expectations of economic agents. Indeed, equation (16) implies

$$z_*(s_*) = s_*(\mathbb{I} - A)^{-1}d = s_*\Big(\frac{b_1}{b_2},\ \frac{b_2 + b_1c_2}{b_2(1-c_1)}\Big)^\top, \quad -\varrho \leqslant s_* \leqslant \varrho, \tag{18}$$

for an equilibrium point $(z_*(s_*), s_*) = (y_*(s_*), x_*(s_*), s_*)$, where $\mathbb{I}$ is the 2×2 identity matrix. Substituting (18) in (17), i.e., setting $z_{t-1} = (y_{t-1}, x_{t-1}) = z_*$ and $s_t = s_{t-1} = s_*$, one obtains

$$(1+\alpha)s_* = \Phi_{\varrho(1+\alpha)}((1+\alpha)s_*),$$

which is satisfied for all $-\varrho \leqslant s_* \leqslant \varrho$. In other words, there is a different equilibrium $(z_*(s_*), s_*)$ for each admissible value of the perception gap variable s_*, i.e., $-\varrho \leqslant s_* \leqslant \varrho$. Thus, the set of all equilibrium points is a closed line segment in the phase space $\mathbb{R}^2 \times [-\varrho, \varrho]$ of the system, see Fig. 2. In particular, the value of the output gap at an equilibrium, $y_*(s_*)$ ranges over the interval $[-\varrho b_1/b_2, \varrho b_1/b_2]$ and the equilibrium value of the actual inflation belongs to the range

$$x_*(s_*) = s_*\frac{b_2 + b_1c_2}{b_2(1-c_1)} \quad \text{with} \quad -\varrho \leqslant s_* \leqslant \varrho.$$

Interestingly, at least in this simple model, the range of equilibrium values of the output gap is unaffected by the controls c_1, c_2 applied by the regulator through Taylor's rule (2). However, these controls do affect the range of possible values of the equilibrium inflation rate.

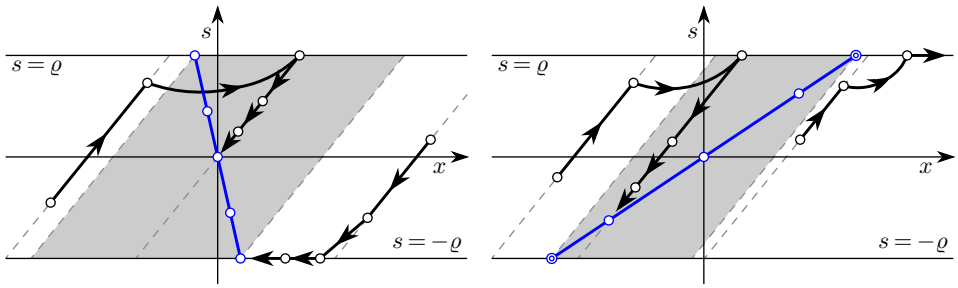

Figure 2. The projection of the line segment of equilibrium points (blue) onto the (x, s) plane for (a) $c_1 > 1$ and (b) $c_1 < 1$. The segment has a negative slope in (a) and a positive slope in (b). Sample trajectories of system (16) are shown in black.

Equation (18) indicates the difference between the cases $c_1 > 1$ and $c_1 < 1$. When $c_1 > 1$, the equilibrium $z_*(\varrho)$ corresponding to the lowest expectation of inflation has

the highest value of the output gap and the lowest inflation of all the equilibrium points. Similarly, the equilibrium $z_*(-\varrho)$ with the highest expectation of inflation has the lowest value of the output gap and the highest inflation. On the other hand, in case $c_1 < 1$, the equilibrium $z_*(\varrho)$ with the highest output gap value has simultaneously the highest inflation rate.

The difference between the cases $c_1 > 1$ and $c_1 < 1$ will be further highlighted in Section 2.5.

2.4. Local stability analysis. System (16), (17) is locally linear in some neighborhood of any equilibrium point from the linear segment (18) with the exception of the two end points $z_*(\pm\varrho)$ corresponding to equilibria where the play is right at one end of its inactive band. More precisely, let us consider the open domain

$$U = \{w = (y, x, s)\colon \|w-(x-s)v_0\|_2 < C(p_{\max}-|x-s|), -p_{\max} < x-s \leqslant p_{\max}\} \tag{19}$$

of the phase space $\mathbb{R}^2 \times [-\varrho, \varrho]$, where

$$\|w\|_2 = \sqrt{x^2 + y^2 + s^2}, \quad p_{\max} = \varrho\frac{b_1c_2 + b_2c_1}{b_2|1 - c_1|}, \tag{20}$$

$$v_0 = \frac{1}{b_1c_2 + b_2c_1}(b_1(1 - c_1), b_2 + b_1c_2, b_2(1 - c_1))^\top \tag{21}$$

and C is defined in Appendix B. One can see that the domain U contains all the internal equilibrium states

$$(z_*(s_*), s_*) = s_*((\mathbb{I} - A)^{-1}d, 1), \quad -\varrho < s_* < \varrho, \tag{22}$$

of the line segment of equilibria given by (18). Moreover, as shown in Appendix B, any trajectory (y_t, x_t, s_t) of dynamical system (16), (17) that starts in U satisfies $x_t - s_t = \text{const}$, i.e., $(y_0, x_0, s_0) \in U$ implies $x_t - s_t = x_0 - s_0$ for all $t \geqslant 1$. Therefore, for such trajectories, equation (16) is equivalent to

$$z_t = Az_{t-1} + (x_t - x_0 + s_0)d, \quad z_t = (y_t, x_t)^\top.$$

Solving for z_t gives the explicit system

$$z_t = Bz_{t-1} - \frac{(x_0 - s_0)\Delta}{1 + a(b_2c_1 + c_2)}d$$

with

$$B = \frac{1}{1 + a(b_2c_1 + c_2)}\begin{pmatrix} 1 & a(b_1 - 1)c_1 \\ b_2 & (1 - b_1)(1 + ac_2) \end{pmatrix}. \tag{23}$$

By inspection, this is equivalent to the iterations

$$z_t - z_*(s_*) = B(z_{t-1} - z_*(s_*)), \quad s_t = x_t - p_0, \quad t \geqslant 1, \tag{24}$$

where

$$p_0 = x_0 - s_0, \quad s_* = \frac{b_2(1-c_1)p_0}{b_1c_2 + b_2c_1}. \tag{25}$$

We further show in Appendix B that the matrix B is stable for any admissible set of parameter values, hence every equilibrium (22) is locally stable. As such, any trajectory (y_t, x_t, s_t) starting in U converges to an equilibrium along the plane $x - s = x_0 - s_0$. The equilibrium $(y_*(s_*), x_*(s_*), s_*) = (z_*(s_*), s_*)$, to which the trajectory converges, is a unique intersection point of the open line segment (22) with the plane $x - s = x_0 - s_0$ defined by the initial condition. Moreover, the two-dimensional dynamics in each slice $\{(y, x, s) \in U\colon\ x - s = x_0 - s_0\}$ of U is linear.

The local stability of equilibrium states ensures that if a *sufficiently small* perturbation is applied to the system residing at an equilibrium $(z_*(s_*), s_*)$, removing the perturbation returns the system to the same equilibrium. Further, the eigenvalues of the matrix B determine how quickly (or slowly) the system returns to the equilibrium state. This situation is of course very similar to the expected response in a fully linear equilibrium model. The dependence of the eigenvalues of the parameters of the system is discussed in Appendix C.

However, the situation for these interior equilibria changes markedly for larger perturbations. This is related to the stability properties of the two extreme equilibria $(z_*(\pm\varrho), \pm\varrho)$ and is far more subtle as discussed in the next subsection. In particular, for $c_1 < 1$, the basin of attraction of the equilibrium decreases and finally vanishes as one approaches either of the extreme equilibrium points along the line segment (18).

2.5. Global stability analysis. System (16) without stickiness ($\varrho = 0$) simply has the form

$$z_t = Az_{t-1}. \tag{26}$$

As shown in Appendix B, its unique zero equilibrium is globally stable if $c_1 > 1$ and is unstable if $c_1 < 1$.

For system (16) with stickiness ($\varrho > 0$), equation (26) approximates the dynamics far from equilibrium points, because the term s_t in (16) is bounded in absolute value by ϱ. In particular, since (26) is unstable for $c_1 < 1$, so is system (16). This creates the possibility of run-away inflation at these values of c_1 (see Section 3.5).

Interestingly, the same condition $c_1 > 1$ that ensures the global stability of system (26) also guarantees the global stability of the set of equilibrium states for the sticky nonlinear system (16). In order to show this, one can use a family of *Lyapunov functions*

$$V(x_t, s_t, \nabla_t x, \nabla_t s) = \frac{1}{2}(C(\nabla_t x)^2 + G(\nabla_t s)^2 + (Cx_t + Gs_t)^2) + \gamma\Big((Cx_t + Gs_t)\nabla_t x + \frac{H}{2C}(Cx_t + Gs_t)^2\Big),$$

where $\nabla_t u = u_t - u_{t-1}$, $u = x, s$. A proper choice of the parameters C, G, H, γ ensures that such a function is nonnegative, achieves its minimum zero value on the linear interval of equilibrium states, and decreases to zero along every trajectory of system (16). This allows us to prove that every trajectory of system (16) converges to one of the equilibrium states (18). Details of the proof can be found in [27].

R e m a r k 3. We see that the parameter c_1 in rate-setting rule (2) is important because for $c_1 < 1$ equilibrium states (possibly, with the exception of end points of the segment) form a local attractor with another attractor at infinity, while for $c_1 > 1$ the segment of equilibrium states is the unique global attractor. In particular, in the case $c_1 < 1$, due to instability of (26), trajectories starting sufficiently far away from equilibrium states tend to infinity. On the other hand, for $c_1 > 1$ each trajectory converges to an equilibrium state. Hence, we observe a global bifurcation at the critical value $c_1 = 1$.

As parameter c_1 *increases* from a small value to 1, the segment of equilibrium states grows longer according to (18). At the bifurcation value $c = 1$, the equilibrium states form the whole straight line $y = s = 0$, $x \in (-\infty, \infty)$. For $c_1 > 1$ the segment of equilibria becomes longer with *decreasing* c_1.

R e m a r k 4. Let us consider system (16), (17) close to the bifurcation point $c_1 = 1$. Let $\lambda_i(c_1)$ be the eigenvalues of the matrix A given by (10). At the bifurcation point, the larger eigenvalue is $\lambda_1(1) = 1$ (with an eigenvector $(0,1)^\top$), the other eigenvalue is $\lambda_2(1) = 1 - b_1 \in (0,1)$. Hence, $\lambda_1(c_1) > 1 > \lambda_2(c_1)$ for $c_1 < 1$ and $1 > \lambda_1(c_1) > \lambda_2(c_1)$ (when c_1 is sufficiently close to 1). Denote by $u(c_1) = (u_1(c_1), u_2(c_1))^\top$ the eigenvector of A, which corresponds to the larger eigenvalue $\lambda_1(c_1)$ and is normalized by the condition

$$\frac{b_2}{\beta}u_1(c_1) + \frac{(1-c_1)ab_2}{\beta}u_2(c_1) = 1. \tag{27}$$

Let us consider iterations (16), (17) starting from the initial point $w_0 = (y_0, x_0, s_0)$ with

$$(y_0, x_0)^\top = z_*(\varrho) + \varepsilon u(c_1), \quad s_0 = \varrho,$$

where $\varepsilon > 0$ and $(z_*(\varrho), \varrho)$ is an end point of the segment of equilibrium states. One can easily conclude by induction that these iterations are given by

$$(y_t, x_t) = z_*(\varrho) + \varepsilon \lambda_1^t(c_1) u(c_1), \quad s_t = \varrho, \quad t \geqslant 0,$$

hence they converge to the equilibrium $(z_*(\varrho), \varrho)$ for $c_1 > 1$ but tend to infinity for $c_1 < 1$. Therefore, the equilibrium $(z_*(\varrho), \varrho)$ is stable for $c_1 > 1$ and unstable for $c_1 < 1$. The same is true for the equilibrium $(z_*(-\varrho), -\varrho)$. Thus, the bifurcation at $c_1 = 1$ changes the stability of the end points of the segment of equilibrium states, while the internal points of this segment remain (locally) stable. Also, by the continuity argument, for $c_1 < 1$ there is an open set of initial conditions, from which trajectories converge to infinity, and the boundary of this open set includes the equilibrium states $(z_*(\pm\varrho), \pm\varrho)$.

For system (9) with noise, this global stability result implies that trajectories tend to return towards the segment of equilibrium points after large fluctuations and hover in a vicinity of equilibrium states for extended periods of time (for $c_1 > 1$). The rate with which the system returns towards the line segment of equilibrium states after a large perturbation is removed is determined by the eigenvalues of the matrix A, see Appendix C. Interestingly, at the bifurcation point $c_1 = 1$, equations for s and y decouple from the equation for x and become

$$s_t = \frac{1}{1+\alpha} \Phi_{\varrho(1+\alpha)} \Big(\frac{b_2}{\beta} y_{t-1} + \alpha s_{t-1} + \frac{b_2}{\beta} \varepsilon_t + \frac{1 + ac_2}{\beta} \eta_t \Big),$$

$$y_t = \frac{y_{t-1}}{1 + ac_2} - \frac{a s_t}{1 + ac_2} + \frac{\varepsilon_t}{1 + ac_2}.$$

Dynamics of such systems was studied in [3].

3. Numerical results

3.1. Parameter values. The default parameter set that we use for numerical simulation is the same as in [12], see Table 1, and we shall explore in detail the surrounding parameter space.

Parameters	a	b_1	b_2	c_1	c_2
Values	0.2	0.5	0.05	1.5	0.5

Table 1. The set of parameter values.

Note that, as an example, if with the above parameters we choose $\varrho = \frac{1}{2}$, then the components of the equilibrium points $z_*(s_*) = (y_*(s_*), x_*(s_*))^\top$ range over the intervals

$$y_*(s_*) \in [-5, 5], \quad x_*(s_*) \in [-6, 6].$$

The choice of ϱ is somewhat arbitrary as there is of course no corresponding reference parameter in [12] and so in many of the simulations it will be varied. Also it should be emphasized that these reference parameters are motivated by [12] but very similar numerical results were obtained for other choices.

3.2. Lower inflation volatility due to stickiness. The range of the equilibrium points of the system is directly proportional to the threshold value ϱ of the play operator, because the perception gap s_* in (18) can take any value in the interval $-\varrho \leqslant s_* \leqslant \varrho$. In particular, $\varrho = 0$ corresponds to the system without stickiness in which the expectation of inflation coincides with the current inflation rate, $p = x$. This system is simply described by the equation

$$z_t = Az_{t-1} + N\xi_t \tag{28}$$

(cf. (9)). In the absence of noise, it has a unique equlibrium at $x = y = 0$.

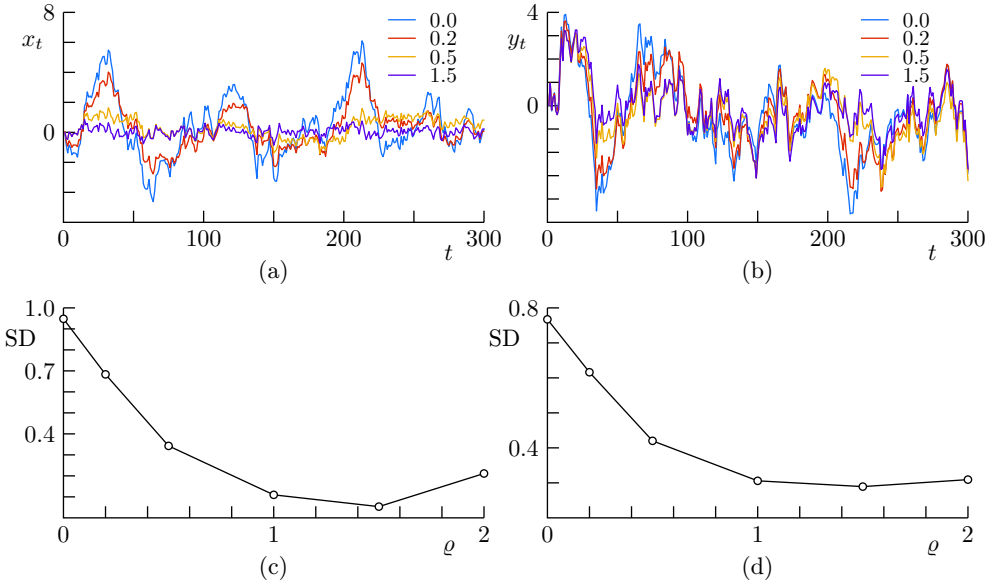

Figure 3. Trajectories of (a) inflation rate x_t and (b) output gap y_t. Measure of volatility of (c) inflation rate and (d) output gap for different values of ϱ with standard deviation (SD).

The sticky system exhibits lower volatility in the inflation rate than the system without stickiness, see Fig. 3. This can be explained by the stability properties of matrices A and B, where B is the linearization matrix of (24) for the sticky system at an equilibrium. For the parameter values of Table 1, the spectral radius of the

matrix B is smaller than the spectral radius of A (see Appendix C), hence the sticky system tries to revert to equilibrium more strongly within the basin of attraction of individual equilibria, i.e. as long as the perception gap does not become extreme. Fig. 3 shows that the volatility decreases with ϱ. For large (compared to ϱ) deviations of z_t from the set of equilibrium points, system (9) behaves as (28).

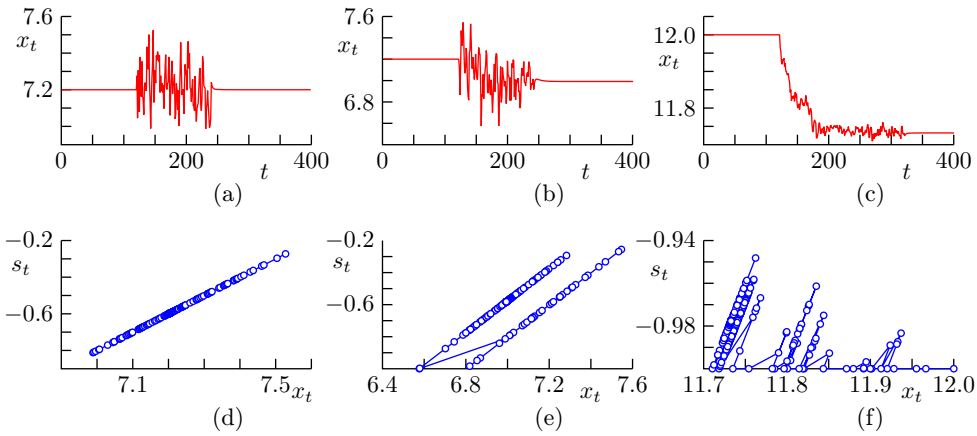

Figure 4. Transitions between the equilibrium states. (a)–(c) Time traces of inflation rate; (d)–(f) the corresponding plots in the (x, s)-space exhibiting different transition scenarios. The noise is turned off before and after the interval of time of interest in order to show the equilibrium state at the ends of this interval. (a), (d) The perception gap remains within the bounds $|s_t| < \varrho$, and the system stays in the basin of attraction of one equilibrium point. The inflation rate $x_*(s_*)$ is the same before and after the noisy interlude. (b), (e) The perception gap reaches the extreme value $-\varrho$ (the highest expectation of inflation), and the trajectory transits from the basin of attraction of an equilibrium state with higher inflation rate and lower output gap (the right slanted segment in (e)) to the basin of attraction of an equilibrium state with a lower inflation rate and higher output gap (the left slanted segment in (e)). (c), (f). A transition from the equilibrium with the highest inflation rate (the rightmost point in (f)) to an equilibrium state with a more moderate inflation rate through the basins of attraction of several other equilibrium states.

3.3. Transitions between equilibrium states. The system remains within the basin of attraction of a particular equilibrium state $z_*(s_*)$ as long as the perception gap s_t does not reach either of the extreme values $\pm\varrho$ and remains confined to the interval $|s_t| < \varrho$, see Fig. 4 (a), (d). But as soon as the perception gap hits the end of its range and starts being 'dragged' by the actual inflation rate (Fig. 4 (b), (e)), the system transitions to the basin of attraction of a different equilibrium state where s_t becomes 'stuck' again. For this reason, the system stays near equilibrium states which correspond to nonextreme perception gaps for longer periods of time than near extreme ones. Figures 4 (c), (f) illustrate a transition from the equilibrium state

with an extreme perception gap, $z_*(\varrho)$, to one with a more moderate perception gap. Higher noise amplitudes promote more often transitions from the basin of attraction of one equilibrium state to another (Fig. 5).

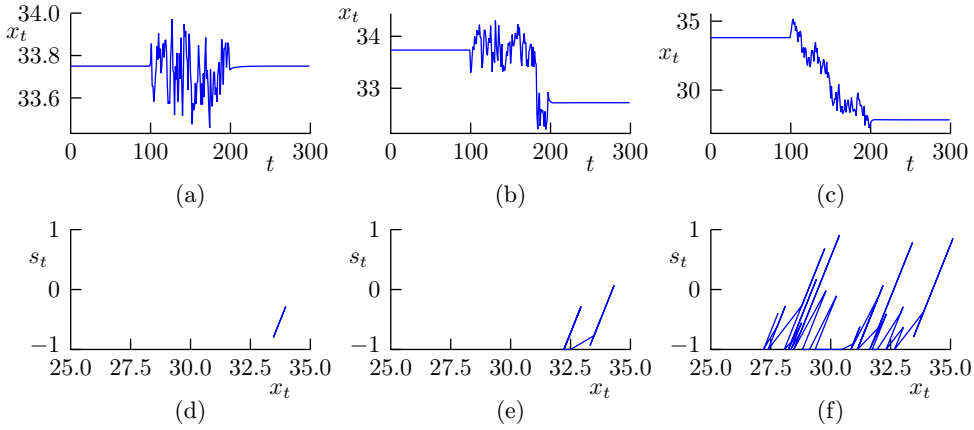

Figure 5. Transitions between the equilibrium states for different noise amplitudes. (a)–(c) Time traces of inflation rate; (d)–(f) the corresponding plots in the (x, s)-space. The noise is turned off before and after the interval of time of interest as in Figure 4. (a), (d) For the noise of amplitude $\sigma = 0.1$, the perception gap remains within the bounds $|s_t| < \varrho$, and the system stays in the basin of attraction of one equilibrium state. The inflation rate $x_*(s_*)$ is the same before and after the noisy interlude. (b), (e) For the noise level $\sigma = 0.25$, the perception gap reaches the extreme value $-\varrho$ once (the highest expectation of inflation), and the trajectory transits from the basin of attraction of an equilibrium state with higher inflation rate and lower output gap (the right slanted segment in (e)) to the basin of attraction of an equilibrium state with a lower inflation rate and higher output gap (the left slanted segment in (e)). (c), (f) For the noise level $\sigma = 0.5$, the perception gap reaches the extreme value $-\varrho$ multiple times and transits from the basin of attraction of one equilibrium to another. The noise is modeled by a sequence of independent Gaussian random variables with zero mean and variance σ^2.

3.4. Response to shocks. We shall stress the system by applying supply shocks through the term η_t. The response of the system to demand shocks applied through the term ε_t is similar. However, the parameter regime being considered diminishes the effect of relatively small demand shocks due to the small value of $b_2 = 0.05$.

System (28) without stickiness, which has a unique globally stable equilibrium state $x_* = y_* = 0$, as expected returns to the equilibrium (and hovers near it due to noise) after each shock, see Fig. 6 (a). Shocks applied to the sticky system (9), (12) result in transitions between equilibrium states, see Figure 6 (b). Numerical simulation shows that shocks of small magnitude typically move the system in the direction of the shock (see Fig. 7 (a)). For example, after a shock that pushes up

the inflation rate, the system settles to a new equilibrium state, which has higher inflation rate (and lower output gap) than the equilibrium occupied prior to the shock. On the other hand, shocks of larger magnitude cause a transition to an equilibrium state that can be hard to predict because such shocks cause a longer and more complex excursion into the phase space far from equilibrium set. In Fig. 7 (b), the system resides near an equilibrium with high inflation rate before a shock is applied. Although the shock pushes the inflation even higher, the system eventually settles to an equilibrium with nearly zero inflation rate after the shock is removed.

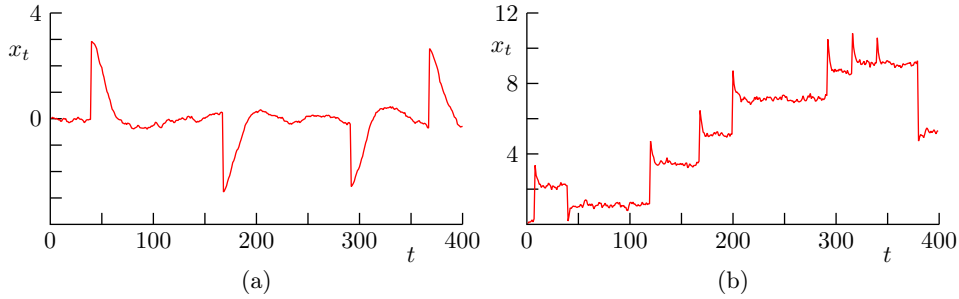

Figure 6. Response to shocks. (a) The system without stickiness ($\varrho = 0$) settles to the same unique equilibrium after each shock. (b) The system with stickiness ($\varrho = 1$) settles to a new equilibrium after a shock is applied.

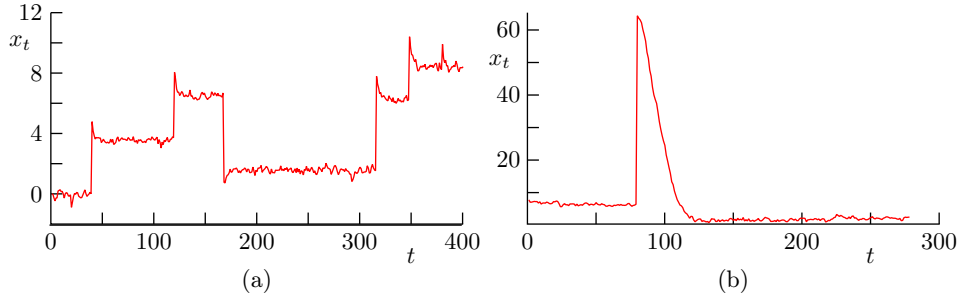

Figure 7. Response to shocks of (a) small and (b) large magnitude.

3.5. The possibility of runaway inflation. According to Section 2.5 the system is globally stable for $c_1 > 1$, but becomes unstable for $c_1 < 1$. The latter case creates a possibility of the run-away inflation scenario. It is interesting that as shown in Section 2.4 all the equilibrium points are *locally* stable even if $c_1 < 1$. As a result, dynamics appear to be stable as long as the trajectory is confined to the basin of attraction of an equilibrium state. However, when noise or a shock or another fluctuation drives the trajectory outside this bounded stability domain, the run-away scenario may and is likely to start, see Fig. 8. Just to be clear, the behavior is stable while the perception gap is not extreme, but if noise or a shock causes

that to change, then the runaway instability can suddenly occur with no change in the system parameters. In particular, the higher the volatility of noise, the faster trajectories leave the domain of attraction of the equilibrium set.

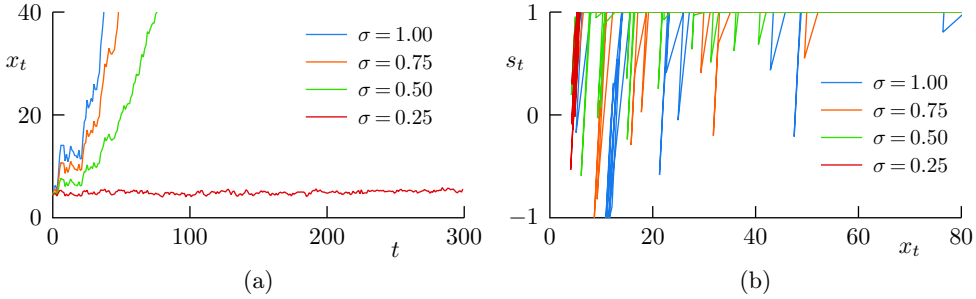

Figure 8. Run-away inflation scenario. Parameters are $\varrho = 1$, $a = 0.3$, $b_1 = 0.5$, $b_2 = 0.05$, $c_1 = 0.9$, $c_2 = 0.01$. The ranges of inflation rate and output gap values at equilibrium states for this set of parameters are $x_* \in [-11, 11]$ and $y_* \in [-10, 10]$, respectively. (a) Time series of inflation rate x_t. (b) Trajectory in the (x, s) space. For the noise amplitude $\sigma = 0.25$, the trajectory stays within the basin of attraction of the equilibrium set over the observation time period. For larger noise amplitudes, the trajectory leaves the domain of attraction to the equilibrium set. The higher the volatility, the faster trajectories leave this domain.

3.6. A trade-off between inflation and output gap volatility. Parameters c_1 and c_2 of Taylor's rule (2) control the volatility level of inflation and output gap near an equilibrium state. Numerical simulations of the model with sticky inflation expectation show that when c_1 increases (which corresponds to stronger inflation targeting by the Central Bank), the volatility of the inflation rate decreases, see Fig. 9 (a). However, at the same time, the output gap becomes highly volatile with increasing c_1, see Fig. 9 (b).

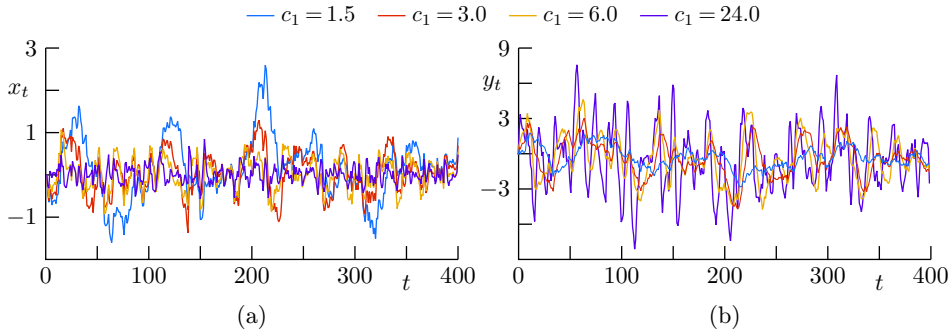

Figure 9. Numerical simulations of (a) inflation rate, x_t and (b) output gap, y_t for $\varrho = 1$ and various values of c_1. The remaining parameters values are from Table 1.

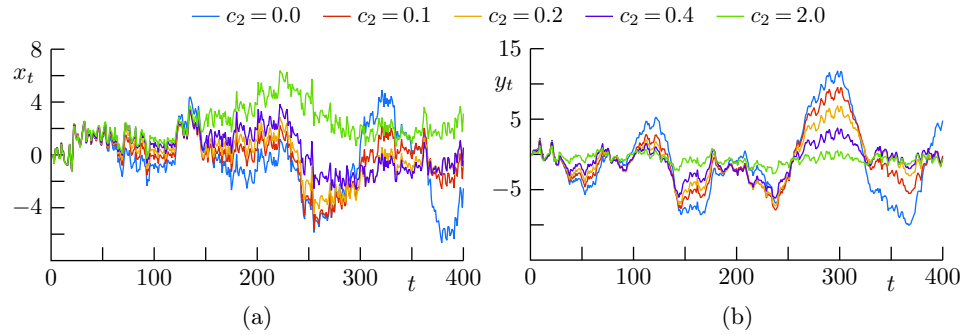

Figure 10. Numerical simulations of (a) inflation rate, x_t and (b) output gap, y_t for $\varrho = 1$ and various values of c_2. The remaining parameter values are from Table 1.

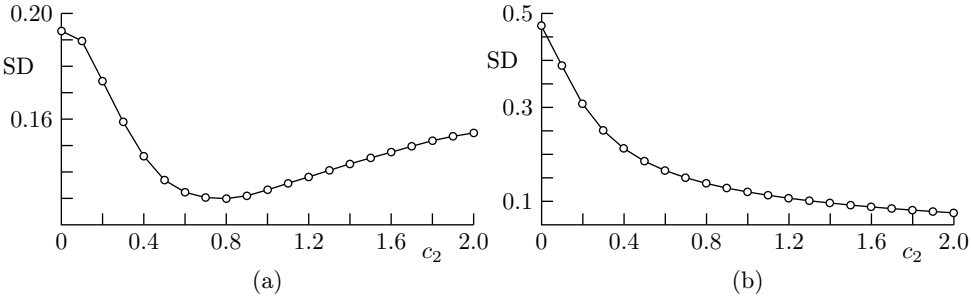

Figure 11. Measure of the effect of c_2 on volatility of (a) x_t and (b) y_t with standard deviation (SD).

When c_2 increases (stronger output gap targeting), the output gap volatility decreases, see Fig. 10 (b). In particular, the case $c_2 = 0$ corresponding to pure inflation targeting in Taylor's rule is characterized by the highest volatility of the output gap. However, from Fig. 10 (a), it appears that the inflation rate volatility exhibits a nonmonotone behavior with c_2. This is confirmed by Fig. 11, which shows the dependence of the standard deviation of x_t and y_t on c_2 for the trajectories presented in Fig. 10. The inflation rate volatility reaches its minimum for $c_2 \approx 0.8$ for the parameter values a, b_1, b_2, c_1 from Table 1 and $\varrho = 1$.

All the above results are in agreement with [12]. In addition, c_1 and c_2 affect the range of the inflation rate value at the equilibrium states for the model (9). According to (18), this range increases with c_2 and decreases with $c_1 - 1$ (for $c_1 > 1$). At the same time, the range of output gap equilibrium values is unaffected by the parameters of Taylor's rule.

3.7. A multi-agent model. Model (9) can be easily extended to account for differing types of agent with different inflation rate expectation rules/thresholds. To

this end, we replace the simple relationship (6) between p_t and x_t with the equation

$$p_t = \sum_{i=1}^{n} \mu_i \mathscr{P}_{\varrho_i}[x_t] = x_t - \sum_{i=1}^{n} \mu_i \mathscr{S}_{\varrho_i}[x_t] \tag{29}$$

with

$$\sum_{i=1}^{n} \mu_i = 1. \tag{30}$$

Here the play operator $\mathscr{P}_{\varrho_i}$ models the expectation of inflation by the ith agent; p_t is the aggregate expectation of inflation; $\mu_i > 0$ is a weight measuring the contribution of agent's expectation of inflation to the aggregate quantity; and, ϱ_i is an individual threshold characterizing the behavior of the ith agent. Relation (29) is equivalent to the formula

$$s_t = \mathcal{I}[x_t] := \sum_{i=1}^{n} \mu_i \mathscr{S}_{\varrho_i}[x_t], \tag{31}$$

which is a (discrete) Prandtl-Ishlinskii (PI) operator with thresholds ϱ_i and weights μ_i [17], [31], [21], where $s_t = x_t - p_t$.

The implicit system (1), (2), (29) with multiple agents can be converted into an explicit form using the same technique as we used for the system with one play operator. Again this involves the inversion of the PI operator. The explicit system

$$z_t = Az_{t-1} + \widehat{\mathcal{I}}[c \cdot z_{t-1} + \widehat{\xi}_t]d + N\xi_t, \tag{32}$$

which is similar to its counterpart (9), includes a PI operator with rescaled thresholds $\widehat{\varrho}_i$ and weights $\widehat{\mu}_i$, see Appendix D for details; ξ_t, $\widehat{\xi}_t$ denote the noise terms.

The stability properties of the equilibrium states of system (32) with multiple agents are similar to the stability properties considered above in Section 2.5. In particular, if we consider the system without external noise for $c_1 > 1$, then the set of equilibrium states is globally stable, and every trajectory converges to an equilibrium state.

In the simulations of this section, we classify economic agents into three categories, strongly, moderately, and weakly sensitive to inflation rate variations (hence $n = 3$), by assigning thresholds $\varrho_1 < \varrho_2 < \varrho_3$, respectively, to these groups, see Fig. 12. Further, the contribution of each group to the aggregate expectation of inflation carries equal weight, $\mu_i = 1/3$.

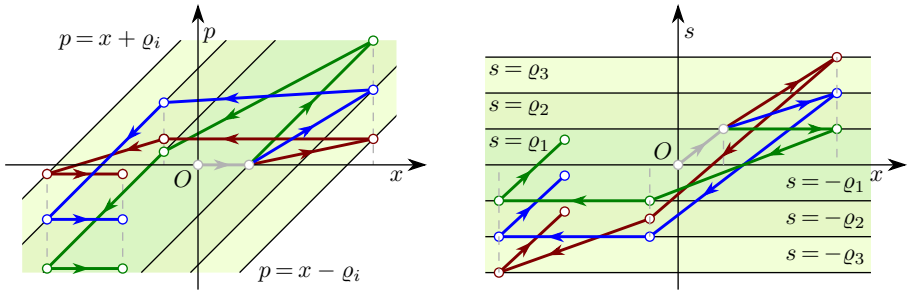

(a) (b)

Figure 12. Different expectations of agents based on three thresholds $\varrho_1 < \varrho_2 < \varrho_3$ of (a) play and (b) stop operators with a single input x_t.

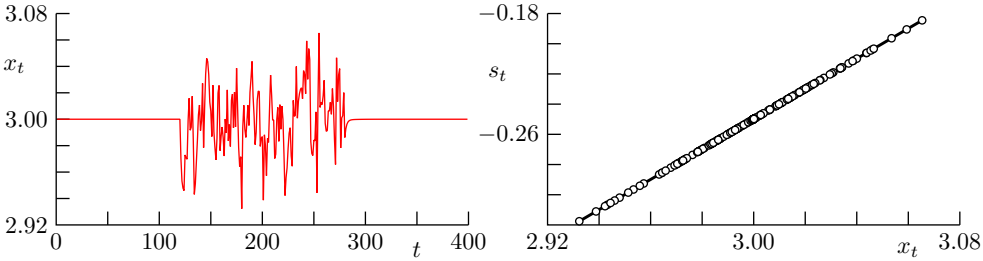

(a) (b)

Figure 13. Trajectory of the system with 3 agents near an equilibrium state when none of the agents achieves an extreme perception gap (cf. Figure 4 (a), (d)). Here $c_1 > 1$. (a) Time trace of inflation. (b) Inflation versus expectation of inflation by any of the agents.

Overall, numerical results obtained for model (1), (2), (29) with three agents are qualitatively similar to the results described above for the model with one agent, see Figs. 13–20, which are counterparts of Figs. 4–11, respectively. Asymmetry of thresholds such as in Remark 1 can be incorporated in this model without difficulty.

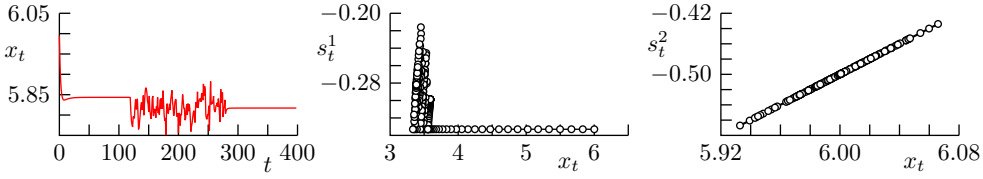

(a) (b) (c)

Figure 14. Trajectory of the system with 3 agents when the most sensitive agent reaches an extreme perception gap but the two less sensitive agents do not (cf. Figure 4 (b), and (e)). The parameter c_1 satisfies $c_1 > 1$. (a) Time trace of inflation. A change of the equilibrium state occurs. (b) Inflation versus expectation of inflation by the most sensitive agent. (c) Inflation versus expectation of inflation by each of the two less sensitive agents.

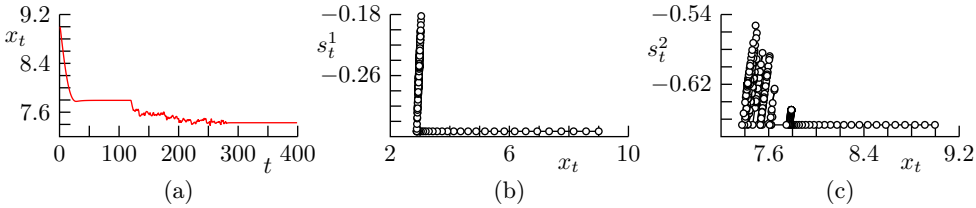

Figure 15. Trajectory of the system with 3 agents with the most sensitive agent and the moderately sensitive agent having an extreme perception gap at the initial (equilibrium) point (cf. Fig. 4 (c), (d)). The parameter c_1 satisfies $c_1 > 1$. (a) Time trace of inflation. (b) Inflation versus expectation of inflation for the moderately sensitive agent. (c) Inflation versus expectation of inflation for the most sensitive agent. The least sensitive agent shows the behavior as in Fig. 14 (c).

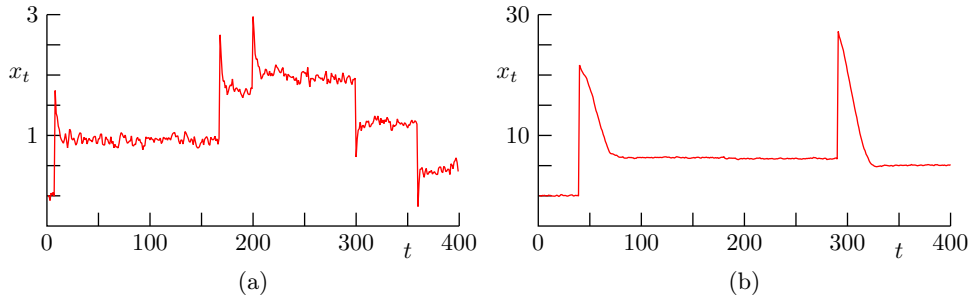

Figure 16. Changes of the equilibrium state in the model with 3 agents due to shocks (cf. Figures 6, 7). (a) Small shocks. (b) Relatively large shocks.

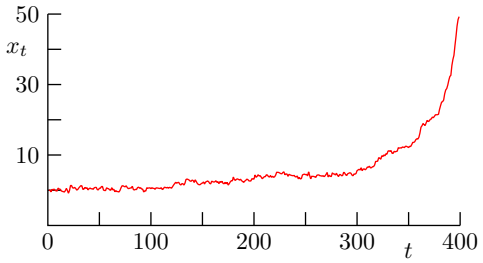

Figure 17. The run-away inflation scenario in the model with 3 agents in the case $c_1 < 1$ (cf. Fig. 8).

3.8. A sticky Central Bank model. The Central Bank policy can presumably exhibit stickiness, too. To explore this scenario in this section we replace the Taylor rule (2) with the relation

$$r_t = \mathcal{P}_\sigma[c_1 x_t + c_2 y_t] \tag{33}$$

also involving a play operator. But at the same time, for the sake of simplicity and in order to isolate the effect of stickiness in the Central Bank response upon the

system, we remove the play operator from equations (1), thus assuming that the aggregate expectation of inflation equals to the current actual inflation rate, $p_t = x_t$; this corresponds to setting $\varrho = 0$ in equations (1). In this case,

$$y_t = y_{t-1} - a(r_t - x_t) + \varepsilon_t, \quad x_t = x_{t-1} + \frac{b_2}{1 - b_1} y_t + \eta_t. \tag{34}$$

It would be interesting to consider the model with both sticky inflation expectation and sticky Central Bank response; however, this is beyond the scope of this paper.

System (33), (34) can be written in the form (9) with

$$s_t = \mathcal{S}_\sigma[c_1 x_t + c_2 y_t],$$

the matrix A defined by (10), $N = A$, and $d = (a(1 - b_1), ab_2)^\top / \Delta$ with Δ defined by (11). The technique presented in Subsection 2.2 can be adapted to convert the implicit system (33), (34) into a well-defined explicit system provided that

$$1 - b_1 - ab_2 > 0 \tag{35}$$

(see Appendix E). Hence, we assume that this condition is satisfied.

Equilibrium states of system (33), (34) with zero noise terms form the line segment

$$(y_*(s_*), x_*(s_*)) = \left(0, \frac{s_*}{c_1 - 1}\right), \quad s_* \in [-\sigma, \sigma]. \tag{36}$$

Notice that the output gap value is zero for all the equilibrium states, while the equilibrium inflation rate ranges over an interval of values. Notably, the local stability analysis (see Appendix E) shows that all the equilibrium states with $s_* \in (-\sigma, \sigma)$ are *unstable* for any set of parameter values. That is, stickiness in the Taylor rule leads to destabilization of equilibrium states.

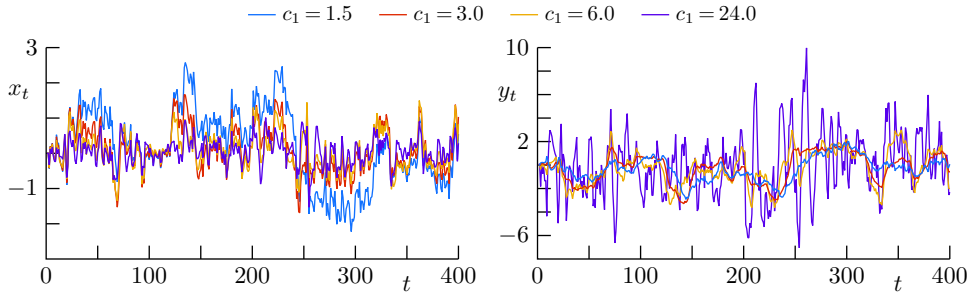

Figure 18. Trade-off between the inflation and output gap volatility in the model with 3 agents as the inflation targeting parameter c_1 in the Taylor rule is varied (cf. Fig. 9). (a) Trajectories of x_t. (b) Trajectories of y_t.

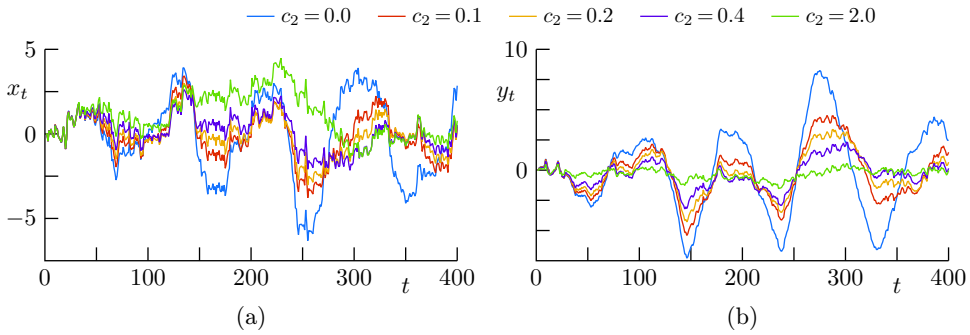

Figure 19. Trade-off between the inflation rate and output gap volatility in the model with 3 agents as the output gap targeting parameter c_2 in the Taylor rule is varied (cf. Fig. 10). (a) Trajectories of x_t. (b) Trajectories of y_t.

On the other hand, for large values of $z_t = (y_t, x_t)^\top$, the system can be approximated by equation (26), which is exponentially stable (as shown in Appendix B). This ensures that in system (33), (34), in the absence of noise, all trajectories converge to a bounded domain Ω surrounding the segment of equilibrium states and, upon entering this domain, remain there. However, since the equilibria are all unstable, more complicated bounded attracting orbits (such as periodic, quasiperiodic, or even chaotic atractors) must occur. Fig. 21 shows a few possibilities for the attractor of system (33), (34) obtained for different sets of parameter values. The attractor belongs to Ω, whose size is controlled by the parameter σ of the sticky Taylor rule (33). This size can be estimated using the Lyapunov function introduced in Subsection 2.5.

Finally, we note that in the presence of noise, a trajectory will most likely wander unpredictably around Ω unless kicked outside temporarily by a fluctuation.

4. Conclusions

In this paper we rigorously analyzed a simple macroeconomic model with sticky inflation expectations. Perhaps surprisingly, although the model is nonlinear, it can be considered as a hybrid (piecewise) linear system and analysed using a mostly linear mathematical toolkit.

For such a simple model, defined via a single (and conceptually quite elementary) change from a standard one, the sticky play operator introduces surprisingly complicated, subtle-yet-recognizable phenomena into the dynamics. Some of the more detailed conclusions of our simulations may be model-specific but, based upon the mathematics presented here and additional numerical simulations with more complex variants of the model, we believe at least the following two qualitative features to be generic and robust.

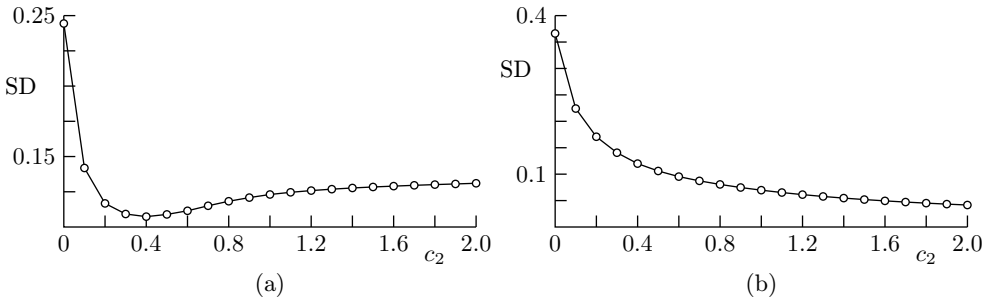

Figure 20. Measure of the effect of c_2 on volatility of (a) inflation rate, x_t and (b) output gap, y_t with standard deviation (SD) (cf. Fig. 11).

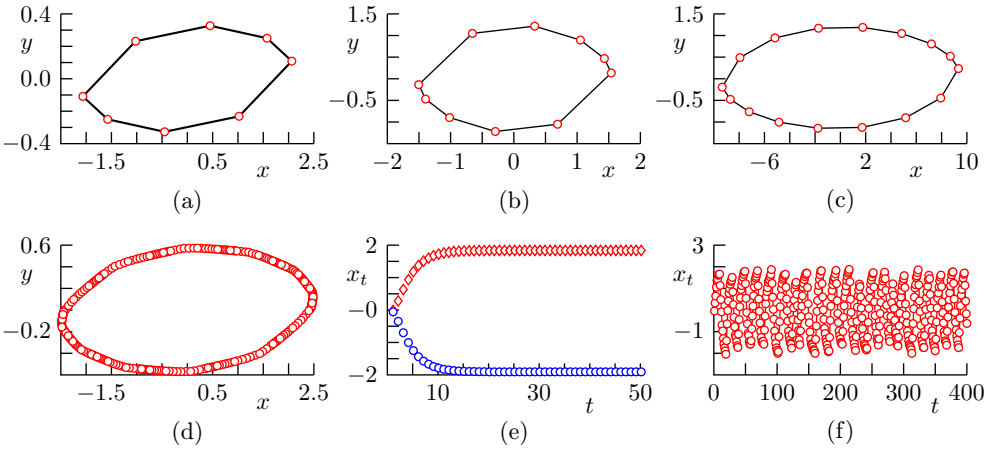

Figure 21. An attractor of system (33), (34) for several parameter sets. (a)–(c) A periodic orbit (with period 8, 10, 16, respectively) shown on the (x, y) plane for the system without noise. (d) A quasiperiodic orbit. (e) Two equilibrium states corresponding to $s_* = \pm\sigma$ (the time trace of x_t shown for 2 trajectories). (f) Time trace of x_t for a trajectory of the system with noise for the same parameters as in (e).

Firstly, the presence of an entire continuum of equilibria rather than a unique one (or even finite numbers of them as occurs in many New-Keynesian models). This causes permanence and path dependence at a deep level. It should be noted that in more sophisticated models, with more variables and more play operators, the set of possible equilibria may be extremely complicated with the possibility of 'cascades' where one play operator starting to drag causes others to do so (the analogy with earthquakes made in Introduction then becomes even closer).

Secondly, the existence of different modes depending upon whether particular play operators are currently 'stuck' or 'dragged'—in our case the 'inner' and 'outer' modes. If some modes are less stable than others (in our main model the outer mode is less stable than the inner one), then a large enough shock may move the system far enough

away from the set of equilibria that the route back to an equilibrium is both long and unpredictable. It may even move the system into an unstable regime—in this case runaway inflation—without any change in the system parameters. Both these features are highly significant not just because they correspond closely to actual economic events but they have implications for forecasting and policy prescriptions too.

Our choice of inflation expectations as the candidate for an initial investigation was influenced by the work of De Grauwe [12] on a different type of boundedly rational expectation formation process in a simple DSGE model. However, play operators are also a viable candidate for modeling other sticky economic variables at both the micro- and macro-economic levels. To demonstrate this, in our final model we used one to represent sticky responses by the Central Bank.

The modeling approach presented above can be thought of as a 'stress test' of the usual rationality assumption in the underlying toy model. Or to put it another way, it is examining the robustness of modeling assumptions rather than just the stability of the solutions within a particular model. As such, we believe that the introduction of a new form of plausible stickiness has intrinsic merit not just as a form of expectation formation. It provides an additional class of perturbed models—ones that are genuinely nonlinear, tractable, and capable of changing solutions (and potentially policy prescriptions) in a way that merely changing the parameters of an equilibrium model cannot.

Our second and third models demonstrated that there are various ways in which this work can be extended, in particular to systems with multiple agents and multiple play operators. Although it has not been relevant to this paper, play and stop operators, when combined appropriately [23], can have a remarkably simple aggregated response, even when connected via a network. This allows for (almost)-analytic solutions even when cascades and rapid transitions between states are occurring and will be the subject of future work.

Appendix

A. Derivation of equations (9), (12). Here we show how to obtain equations (9), (12) from model (1)–(4). To this end, we substitute the equation for r_t into the equation for y_t and obtain

$$(1 + ac_2)y_t = y_{t-1} - ac_1x_t + ap_t + \varepsilon_t.$$

Next, we substitute this equation into the equation for x_t and simplify to obtain

$$\gamma x_t - \beta p_t = b_2y_{t-1} + (1 - b_1)(1 + ac_2)x_{t-1} + b_2\varepsilon_t + (1 + ac_2)\eta_t, \tag{37}$$

where β is defined in (13) and

$$\gamma = 1 + ac_2 + ab_2c_1.$$

Since $p_t = x_t - s_t$, equation (37) can be rewritten as

$$\alpha x_t + s_t = f_t \tag{38}$$

with α and f_t defined by (13), (15). Therefore, $x_t = \alpha^{-1}(f_t - s_t)$, which combined with (13), (15) gives

$$x_t = \frac{b_2}{\Delta}y_{t-1} + \frac{(1-b_1)(1+ac_2)}{\Delta}x_{t-1} - \frac{1}{\alpha}s_t + \frac{b_2}{\Delta}\varepsilon_t + \frac{1+ac_2}{\Delta}\eta_t, \tag{39}$$

where $\Delta = \alpha\beta$, see (11). Subsequently, substituting equation (39) into equation (4) gives

$$\begin{aligned} y_t = {} & \frac{ab_2(1-c_1)+\Delta}{\Delta(1+ac_2)}y_{t-1} + \frac{a(1-c_1)(1-b_1)}{\Delta}x_{t-1} \\ & + \frac{a(c_1-1-\alpha)}{\alpha(1+ac_2)}s_t + \frac{\Delta+ab_2(1-c_1)}{\Delta(1+ac_2)}\varepsilon_t + \frac{a(1-c_1)}{\Delta}\eta_t. \end{aligned} \tag{40}$$

Equations (39), (40) can be written as system (9) with the matrices A, N and the vector d defined by formulas (10).

Furthermore, substituting (39) in (7) gives

$$s_t = \Phi_\varrho\Big(-\frac{s_t}{\alpha} + w_t + s_{t-1} - x_{t-1}\Big),$$

where we denote

$$w_t = \frac{b_2}{\Delta}y_{t-1} + \frac{(1-b_1)(1+ac_2)}{\Delta}x_{t-1} + \frac{b_2}{\Delta}\varepsilon_t + \frac{1+ac_2}{\Delta}\eta_t. \tag{41}$$

Equivalently, introducing the notation

$$u_t = -\frac{s_t}{\alpha} + w_t + s_{t-1} - x_{t-1}, \tag{42}$$

we obtain

$$\alpha(w_t + s_{t-1} - x_{t-1}) = \Phi_\varrho(u_t) + \alpha u_t.$$

By inspection, the function $(\Phi_\varrho + \mathbb{I})(u) = \Phi_\varrho(u) + \alpha u$ is invertible and its inverse equals

$$(\Phi_\varrho + \mathbb{I})^{-1}(u) = \frac{u}{\alpha} - \frac{1}{\alpha(1+\alpha)}\Phi_{\varrho(1+\alpha)}(u),$$

hence

$$u_t = w_t + s_{t-1} - x_{t-1} - \frac{1}{\alpha(1+\alpha)}\Phi_{\varrho(1+\alpha)}(\alpha(w_t + s_{t-1} - x_{t-1})).$$

Due to (42), this is equivalent to

$$s_t = \frac{1}{(1+\alpha)}\Phi_{\varrho(1+\alpha)}(\alpha w_t + \alpha s_{t-1} - \alpha x_{t-1}), \tag{43}$$

which, combined with (41), implies (12). This completes the derivation of the explicit system (9), (12).

Since equations (15) and (41) imply $f_t = \alpha w_t$ and (38) implies $\alpha x_{t-1} = f_{t-1} - s_{t-1}$, equation (43) is also equivalent to (14). Alternatively, equation (14) can be obtained from relation (38) using the inversion formula for the play operator. This inversion formula is presented for a more general Prandtl-Ishlinskii (PI) operator, including the play operator as a particular case, in Appendix D.

B. Local stability analysis. First, let us consider the system without stiction. The characteristic polynomial of matrix A is

$$P_A(\lambda) = \Delta\lambda^2 - (1-b_1)(2+ac_2)\lambda + 1 - b_1$$

with Δ defined by (11). Applying Jury's stability criterion, we obtain

$$\begin{aligned} P_A(1) &= 1 - \frac{(1-b_1)(2+ac_2)}{\Delta} + \frac{1-b_1}{\Delta} > 0, \\ P_A(-1) &= 1 + \frac{(1-b_1)(2+ac_2)}{\Delta} + \frac{1-b_1}{\Delta} > 0, \quad 1 > \frac{1-b_1}{\Delta}. \end{aligned}$$

Taking into account the constraints $a, b_2, c_1, c_2 > 0$ and $0 < b_1 < 1$, these conditions result in the relationship

$$c_1 > 1.$$

Note that the system $z_t = Az_{t-1}$ is the linearization of sticky system (9) at infinity, hence it describes the return of the sticky system towards near equilibrium dynamics after a large perturbation. Thus, the stability condition $c_1 > 1$ for A agrees with the global stability criterion obtained in Section 2.5.

Now, let us consider local stability of equilibrium states. Define the open domain

$$\Omega = \{w = (y, x, s) \in \mathbb{R}^2 \times [-\varrho, \varrho] \colon\ |(n \cdot w)| < (1+\alpha)\varrho\},$$

where

$$n = \frac{1}{\beta}(b_2, (1-c_1)ab_2, \Delta)^\top \tag{44}$$

and $w \cdot u = w_1 \cdot u_1 + w_2 \cdot u_2 + w_3 \cdot u_3$ is the standard scalar product in the phase space. Note that the set Ω contains all the equilibrium states (22) of system (16), (17)

(i.e., all the internal points of the whole segment of equilibrium states). Since $\Phi_{\varrho(1+\alpha)}(x) = x$ for $|x| \leqslant (1+\alpha)\varrho$, equations (17) and (39), (40) imply that for $(y_{t-1}, x_{t-1}, s_{t-1}) \in \Omega$,

$$(y_t, x_t, s_t)^\top = M(y_{t-1}, x_{t-1}, s_{t-1})^\top \tag{45}$$

with

$$M = \frac{1}{1 + a(b_2c_1 + c_2)} \begin{pmatrix} 1 & a(1-c_1) & a(b_1c_1 - 1) \\ b_2 & 1 + a(b_2 + c_2) & -(b_1 + ab_2 + ab_1b_2) \\ b_2 & ab_2(1-c_1) & 1 + a(b_1(c_1-1) + c_2) - b_1(1 + ac_2) \end{pmatrix}.$$

Consequently,

$$x_t - s_t = x_{t-1} - s_{t-1}, \quad (y_{t-1}, x_{t-1}, s_{t-1}) \in \Omega, \tag{46}$$

which means that each trajectory in Ω is restricted to a plane $x - s = \text{const}$. By inspection, the restriction of (45) to a plane $x - s = \text{const}$ is given by system (24) with the matrix B defined by (23). Moreover, it follows that the matrix M has the eigenvalue $\lambda_0 = 1$, and the corresponding eigenvector is (21). Therefore, the characteristic polynomial of M has the form $P_M(\lambda) = (\lambda - 1)P_B(\lambda)$, where

$$P_B(\lambda) = \lambda^2 - \lambda\Big(\frac{2 + ac_2 - b_1(1 + ac_2)}{1 + a(b_2c_1 + c_2)}\Big) + \frac{1 - b_1}{1 + a(b_2c_1 + c_2)}$$

is the characteristic polynomial of matrix (23). Applying Jury's stability criterion to $P_B(\lambda)$ gives the following set of inequalities:

$$P_B(1) = 1 - \frac{2 + ac_2 - b_1(1 + ac_2)}{1 + a(b_2c_1 + c_2)} + \frac{1 - b_1}{1 + a(b_2c_1 + c_2)} > 0,$$
$$P_B(-1) = 1 + \frac{2 + ac_2 - b_1(1 + ac_2)}{1 + a(b_2c_1 + c_2)} + \frac{1 - b_1}{1 + a(b_2c_1 + c_2)} > 0, \quad 1 > \frac{1 - b_1}{1 + a(b_2c_1 + c_2)}.$$

It is easy to see that all the three inequalities above are satisfied for any set of parameters $a, b_2, c_1, c_2 > 0$ and $0 < b_1 < 1$. Hence, we conclude that each equilibrium state (22) is stable and locally attracting, the dynamics in a sufficiently small neighborhood of any such state is linear and satisfies $x_t - s_t = \text{const}$.

We proceed to construct an explicit open domain $U \subset \Omega$ of the form (19) such that

(i) U contains the open segment of equilibrium states (22);
(ii) $w_0 = (y_0, x_0, s_0) \in U$ implies

$$w_t = (y_t, x_t, s_t) \in \Omega, \quad t \geqslant 1. \tag{47}$$

Due to (ii), for $(y_0, x_0, s_0) \in U$, the iterations (y_t, x_t, s_t) satisfy (46) and converge to the equilibrium $(z_*(s_*), s_*)$ defined by (18), (25). Equivalently,

$$w_t = (y_t, x_t, s_t) \to (x_0 - s_0)v_0 \quad \text{as } t \to \infty, \tag{48}$$

where v_0 is given by (21).

Theorem 1. *There exists a $C > 0$ such that the trajectory of system* (16), (17) *satisfies* (45)–(48) *for each initial condition $w_0 = (y_0, x_0, s_0) \in U$ from the domain U defined by* (19).

The constant $C > 0$ is found explicitly in the following lemmas, which distinguish between the cases when the eigenvalues λ_1, λ_2 of the matrix B are real and complex.

For every $p \in \mathbb{R}$, the intersection of the boundary $\partial\Omega$ of the domain Ω with the plane $x - s = p$ consists of the two parallel straight lines $l_p^{\pm}$. By inspection, the minimum of the two distances $\operatorname{dist}(pv_0, l_p^+)$ and $\operatorname{dist}(pv_0, l_p^-)$ equals

$$\kappa(p) = \Big|1 - \frac{b_2|1 - c_1||p|}{b_1c_2 + b_2c_2}\Big| \frac{(1+\alpha)\varrho\|n'\|_2}{|n \cdot n'|}, \tag{49}$$

where n is given by (44) and

$$n' = \frac{1}{2\beta}(2b_1,\ (1-c_1)ab_2 + \alpha,\ (1-c_1)ab_2 + \alpha)^\top.$$

Lemma 1. *Let the matrix B have real eigenvalues $\lambda_1 \neq \lambda_2$. Let v_1, v_2 be eigenvectors of M corresponding to its eigenvalues λ_1, λ_2, respectively, and let φ be the angle between v_1 and v_2. Then*

$$\|w_0 - (x_0 - s_0)v_0\|_2 \leqslant \frac{1}{2}|\sin\varphi|\kappa(x_0 - s_0) \tag{50}$$

implies (46), (47) *and*

$$\|w_t - (x_0 - s_0)v_0\|_2 \leqslant \kappa(x_0 - s_0), \quad t \geqslant 1. \tag{51}$$

P r o o f. Since v_1 and v_2 belong to the plane $0 = x - s$, we have the decomposition

$$w_0 = (x_0 - s_0)v_0 + C_1v_1 + C_2v_2. \tag{52}$$

Let us show (51) by induction provided (50) holds. The base case is obvious. For the induction step, assume that $w_\tau \in \Omega$ and $x_\tau - s_\tau = x_0 - s_0$ for $0 \leqslant \tau < t$, therefore using (45), we obtain

$$w_t = (x_0 - s_0)v_0 + C_1\lambda_1^t v_1 + C_2\lambda_2^t v_2,$$

and due to $|\lambda_i| \leqslant 1$,

$$\|w_t - (x_0 - s_0)v_0\|_2 = \|C_1\lambda_1^t v_1 + C_2\lambda_2^t v_2\|_2 \leqslant |C_2|\|v_1\|_2 + |C_2|\|v_2\|_2. \tag{53}$$

From relations (50) and (52), it follows that

$$\frac{1}{2}|\sin\varphi|\kappa(x_0 - s_0) \geqslant \|C_1v_1 + C_2v_2\|_2 \geqslant \|C_1v_1\|_2|\sin\varphi|,$$
$$\frac{1}{2}|\sin\varphi|\kappa(x_0 - s_0) \geqslant \|C_1v_1 + C_2v_2\|_2 \geqslant \|C_2v_2\|_2|\sin\varphi|,$$

therefore (53) implies (51). Finally, (45) implies $x_t - s_t = x_0 - s_0$, hence, by definition of $\kappa(x_0 - s_0)$, (51) implies $w_t \in \Omega$, which concludes the induction step. □

Lemma 2. *Let the matrix B have complex eigenvalues $\lambda_1 = \bar{\lambda}_2$. Let $v_1 = u_1 + \mathrm{i}u_2$ be a complex eigenvector of the matrix M corresponding to its eigenvalue λ_1, and let φ be the angle between the real vectors u_1 and u_2. Then*

$$\|w_0 - (x_0 - s_0)v_0\|_2 \leqslant \frac{\|u_1\|_2\|u_2\|_2}{\|u_1\|_2^2 + \|u_2\|_2^2}|\sin\varphi|\kappa(x_0 - s_0) \tag{54}$$

implies (46), (47) *and* (51).

P r o o f. The proof is obtained by a slight modification of the proof of Lemma 1 above. Since u_1 and u_2 belong to the plane $0 = x - s$, we have the decomposition

$$w_0 = (x_0 - s_0)v_0 + \Re e((C_1 - \mathrm{i}C_2)(u_1 + \mathrm{i}u_2)) \tag{55}$$

with real C_1, C_2. Assuming that $w_\tau \in \Omega$ and $x_\tau - s_\tau = x_0 - s_0$ for $0 \leqslant \tau < t$ and using (45), we obtain

$$w_t = (x_0 - s_0)v_0 + \Re e(\lambda_1^t(C_1 + \mathrm{i}C_2)(u_1 + \mathrm{i}u_2))$$

and due to $|\lambda_1| \leqslant 1$,

$$\|w_t - (x_0 - s_0)v_0\|_2 \leqslant \sqrt{(C_1^2 + C_2^2)(\|u_1\|_2^2 + \|u_2\|_2^2)}. \tag{56}$$

Relations (54), (55) imply

$$\begin{aligned}\frac{\|u_1\|_2\|u_2\|_2}{\|u_1\|_2^2 + \|u_2\|_2^2}|\sin\varphi|\kappa(x_0 - s_0) &\geqslant \|C_1u_1 + C_2u_2\|_2 \\ &\geqslant |\sin\varphi|\max\{\|C_1u_1\|_2, \|C_2u_2\|_2\}.\end{aligned}$$

Combining this with (56), one obtains (51). □

Lemma 3. *Let the matrix B have a double eigenvalue $\lambda_1 = \lambda_2$. Let v_1 and v_2 be, respectively, an eigenvector and a generalized eigenvector of the matrix M corresponding to its double eigenvalue λ_1, and let v_1 and v_2 be orthogonal. If $0 < \lambda_1 \leqslant 1/\mathrm{e}$, then*

$$\|w_0 - (x_0 - s_0)v_0\|_2 \leqslant \frac{\|v_2\|_2}{\|v_1\|_2 + 2\|v_2\|_2}\kappa(x_0 - s_0) \tag{57}$$

implies (46), (47) *and* (51). *If $\lambda_1 > 1/\mathrm{e}$, then*

$$\|w_0 - (x_0 - s_0)v_0\|_2 \leqslant \frac{\mathrm{e}|\ln\lambda_1|\|v_2\|_2}{\|v_1\|_2 + 2\mathrm{e}|\ln\lambda_1|\|v_2\|_2}\kappa(x_0 - s_0) \tag{58}$$

implies (46), (47) *and* (51).

P r o o f. As in the proof of Lemma 1, assuming that $w_\tau \in \Omega$ and $x_\tau - s_\tau = x_0 - s_0$ for $0 \leqslant \tau < t$ and using decomposition (52), we obtain

$$w_t = (x_0 - s_0)v_0 + (C_1\lambda_1^t + tC_2\lambda_1^{t-1})v_1 + C_2\lambda_1^t v_2.$$

Let us notice that if $\lambda_1 \leqslant 1/\mathrm{e}$, then the derivative of function $f(t) = t\lambda_1^t$ satisfies

$$f'(t) = \lambda_1^t + \ln(\lambda_1)t\lambda_1^t \leqslant \lambda_1^t(1 - t) \leqslant 0, \quad t \geqslant 1.$$

In this case, using $f(t) \leqslant f(1)$ and $|\lambda_1| \leqslant 1$, we obtain for $t \geqslant 1$

$$\|w_t - (x_0 - s_0)v_0\|_2 \leqslant |C_1|\|v_1\|_2 + |C_2|(\|v_1\|_2 + \|v_2\|_2). \tag{59}$$

But (57) implies

$$\frac{\|v_2\|_2}{\|v_1\|_2 + 2\|v_2\|_2}\kappa(x_0 - s_0) \geqslant \|C_1v_1 + C_2v_2\|_2 \geqslant \max\{\|C_1v_1\|_2, \|C_2v_2\|_2\},$$

which, when combined with (59), gives (51).

On the other hand, if $1/\mathrm{e} < \lambda_1 < 1$, then the function $f(t) = t\lambda_1^t$ achieves its maximum $f(t_m) = -1/(\mathrm{e}\ln(\lambda_1))$ on the semi-axis $t \geqslant 0$ at $t_m = -1/\ln(\lambda_1)$. Hence, in this case,

$$\|w_t - (x_0 - s_0)v_0\|_2 \leqslant |C_1|\|v_1\|_2 + |C_2|\Big(\frac{\|v_1\|_2}{\mathrm{e}|\ln(\lambda_1)|} + \|v_2\|_2\Big).$$

If (58) holds, then

$$\frac{\mathrm{e}|\ln\lambda_1|\|v_2\|_2}{\|v_1\|_2 + 2\mathrm{e}|\ln\lambda_1|\|v_2\|_2}\kappa(x_0 - s_0) \geqslant \|C_1v_1 + C_2v_2\|_2 \geqslant \max\{\|C_1v_1\|_2, \|C_2v_2\|_2\},$$

consequently (51) is valid. □

Define

$$C_0 = \frac{(1+\alpha)\varrho b_2|1-c_1|\|n'\|_2}{(b_1c_2+b_2c_1)|n\cdot n'|}.$$

According to the above lemmas, the conclusion of Theorem 1 holds if the constant C in the definition of the domain (19) is equal to $C = C_0|\sin\varphi|/2$ under the conditions of Lemma 1, $C = C_0\|u_1\|_2\|u_2\|_2|\sin\varphi|/(\|u_1\|_2^2 + \|u_2\|_2^2)$ under the conditions of Lemma 2, $C = C_0\|v_2\|_2/(\|v_1\|_2 + 2\|v_2\|_2)$ under the conditions of Lemma 3 if $\lambda_1 \leqslant 1/\mathrm{e}$, and $C = C_0\mathrm{e}|\ln\lambda_1|\|v_2\|_2/(\|v_1\|_2 + 2\mathrm{e}|\ln\lambda_1|\|v_2\|_2)$ under the conditions of Lemma 3 if $\lambda_1 > 1/\mathrm{e}$.

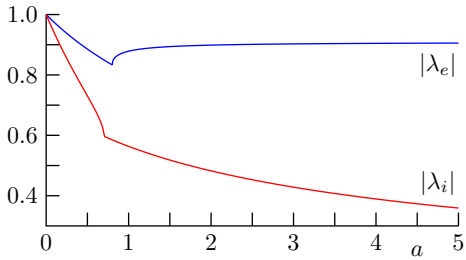

Figure 22. Variation of $|\lambda_i|$ and $|\lambda_e|$ with a. Other parameters are taken from Table 1.

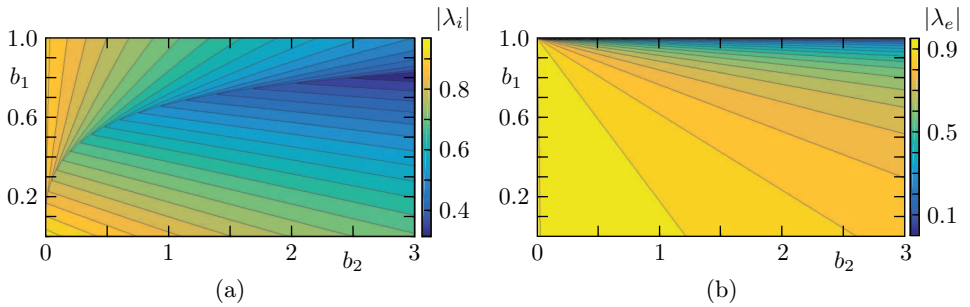

Figure 23. Dependence of (a) $|\lambda_i|$ and (b) $|\lambda_e|$ on b_1 and b_2. Other parameters are taken from Table 1.

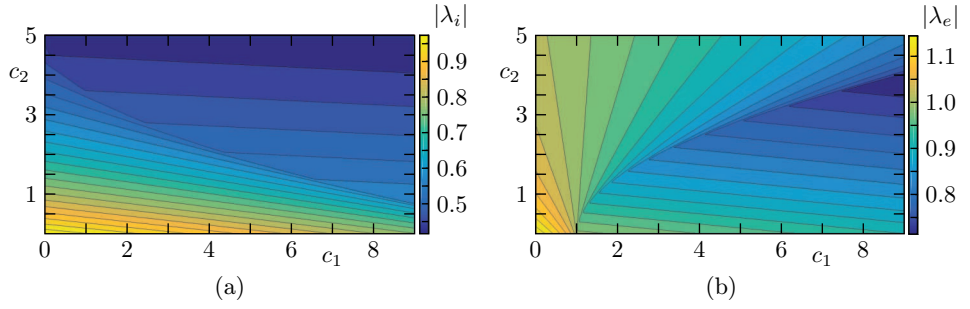

Figure 24. Dependence of (a) $|\lambda_i|$ and (b) $|\lambda_e|$ on c_1 and c_2. Other parameters are taken from Table 1.

C. The effect of parameters on stability properties. Here we provide a numerical analysis concerning the effect of the parameters on stability properties of the equilibrium states. Stronger stability generally implies lower volatility and more infrequent transitions between different equilibrium states. We quantify local stability using the maximum absolute value, $|\lambda_{i,e}|$, of eigenvalues of the linearized system at an equilibrium point. The subscripts e and i refer to the system without stickiness ($\varrho = 0$) and with stickiness ($\varrho = 1$), respectively.

The model contains five other parameters, a, b_1, b_2, c_1 and c_2. Fig. 22 shows the dependence of $|\lambda_{i,e}|$ on the parameter a and implies that the system with stickiness is more stable than the system without stickiness. Other parameter values are taken from Table 1. Interestingly, the system with stickiness becomes more stable for increasing a, while this dependence for the nonsticky system is nonmonotone since $|\lambda_e|$ has a minimum at $a \approx 0.8$.

The range of output gap equilibrium values is proportional to the ratio of parameters b_1 and b_2 according to (18). Fig. 23 presents the dependence of $|\lambda_{i,e}|$ on these parameters. The sticky system is more stable than its nonsticky counterpart for $b_1 < 0.9$, but becomes less stable than the nonsticky system as b_1 approaches 1 (in the latter case, the future inflation rate is defined predominantly by expectations). The dependence of $|\lambda_{i,e}|$ on b_2 and the dependence of $|\lambda_e|$ on b_1 is monotone (stronger stability for larger $b_{1,2}$), while the dependence of $|\lambda_i|$ on b_2 is nonmonotone. The strongest stability is achieved by the sticky system for some intermediate value of b_1 between 0 and 1.

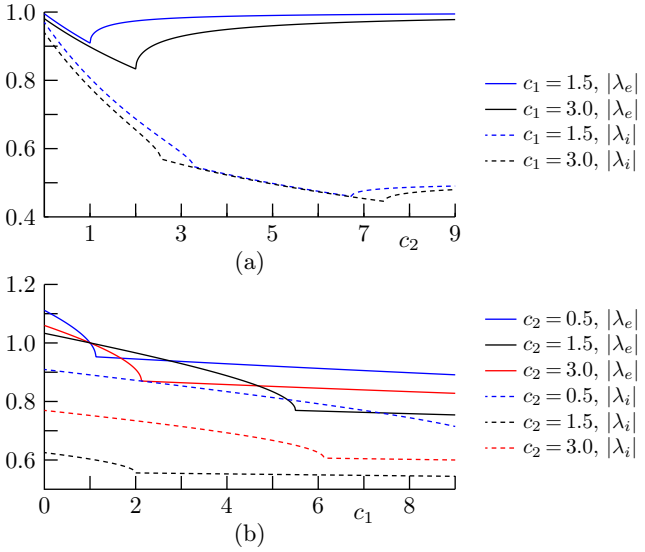

Figure 25. Cross sections of the plots shown in Fig. 24 (a) for various c_2 values and (b) for various c_1 values.

Parameters c_1 and c_2 control the range of inflation rate equilibrium values according to (18). This range contracts when c_1 increases (for $c_1 > 1$) and expands when c_2 increases. Fig. 24 shows that the sticky system is generally more stable than the nonsticky one. Both systems become more stable with increasing c_1 (stronger inflation targeting in Taylor's rule), see Figs. 24 (a), (b) and 25 (a), (b). The dependence of $|\lambda_i|$ on c_2 demonstrates some slight nonmonotonicity for large c_2 values, see Figure 25 (b). The nonmonotonicity of $|\lambda_i|$ with c_2 is much more pronounced with the minimum achieved for a certain value of c_2 depending on c_1, see Figs. 24 (b) and 25 (b). This minimum corresponds to the strongest stability and, in this sense, optimizes the Central Bank policy. In Fig. 24 (b), the strongest stability is achieved on the 'parabolic' line.

D. Inversion of the PI operator. In this section, we consider the inversion of the PI operator, which is necessary to transform the implicit system (1), (2) coupled with relation (29) into the explicit form (32). Here we use the term 'PI operator' for an input-output relationship of the form

$$f_t = \alpha x_t + \sum_{i=1}^{n} \mu_i \mathscr{S}_{\varrho_i}[x_t], \tag{60}$$

where the weights μ_i are allowed to have any sign, $\alpha \geqslant 0$, and $\varrho_1 < \varrho_2 < \ldots < \varrho_n$. Such an operator is completely defined by the so-called *Primary Response* (PR) *function* $\varphi(x)$, which describes the output in response to a monotonically increasing input.

Here, this is a piecewise linear continuous function satisfying $\varphi(0) = 0$ with the slopes defined by

$$\varphi'(x) = \begin{cases} \alpha + \mu_n + \ldots + \mu_2 + \mu_1, & 0 < x < \varrho_1, \\ \alpha + \mu_n + \ldots + \mu_2, & \varrho_1 < x < \varrho_2, \\ \vdots & \\ \alpha + \mu_n, & \varrho_{n-1} < x < \varrho_n, \\ \alpha, & x > \varrho_n, \end{cases}$$

see Fig. 26. As shown in [22], if the slopes of φ are all positive, then the PI operator (60) is invertible, and the inverse relationship is also a PI operator:

$$x_t = \widehat{\alpha} f_t + \sum_{i=1}^{n} \widehat{\mu}_i \mathscr{S}_{\widehat{\varrho}_i}[f_t]. \tag{61}$$

Further, the PR function of operator (61) is the inverse of the PR function φ of operator (60). This allows one to express the weights $\widehat{\alpha}$, $\widehat{\mu}_i$ and the thresholds $\widehat{\varrho}_i$

explicitly in terms of the weights α, μ_i and the thresholds ϱ_i. In particular, the equation $\alpha x_t + s_t = f_t$ with $s_t = \mathcal{S}_\varrho[x_t]$ (see (38)) can be inverted as

$$x_t = \frac{1}{\alpha} f_t - \frac{1}{\alpha(1+\alpha)} \mathcal{S}_{(1+\alpha)\varrho}[f_t],$$

and this implies $s_t = (1+\alpha)^{-1} \mathcal{S}_{(1+\alpha)\varrho}[f_t]$, which is equivalent to (14) (cf. Appendix A).

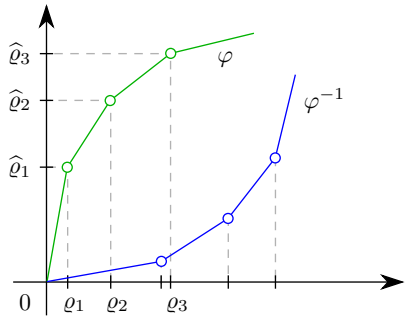

Figure 26. PR function φ of PI operator (60) and PR function φ^{-1} of its inverse PI operator (61).

E. Sticky Taylor rule. In order to convert system (33), (34) to the explicit form, we replace the variable y_t with the variable $g_t = c_1 x_t + c_2 y_t$ and obtain

$$g_t = (c_1 + ac_2)x_t + g_{t-1} - c_1 x_{t-1} - ac_2 \mathscr{P}_\sigma[g_t] + c_2 \varepsilon_t, \tag{62}$$

$$x_t = \frac{c_2(1-b_1)}{b_2 c_1 + c_2(1-b_1)} x_{t-1} + \frac{b_2}{b_2 c_1 + c_2(1-b_1)} g_t + \frac{c_2(1-b_1)}{b_2 c_1 + c_2(1-b_1)} \eta_t. \tag{63}$$

Further, substituting (63) into (62) gives

$$\alpha g_t + \kappa \mathscr{P}_\sigma[g_t] = f_t \tag{64}$$

with

$$\alpha = \frac{c_2(1-b_1-ab_2)}{b_2 c_1 + c_2(1-b_1)}, \quad \kappa = ac_2,$$
$$f_t = g_{t-1} - c_1 x_{t-1} + \frac{c_2(1-b_1)(c_1+ac_2)}{b_2 c_1 + c_2(1-b_1)}(x_{t-1} + \eta_t) + c_2 \varepsilon_t.$$

Using that $\alpha > 0$ due to (35), we can invert (64) as in Appendix D to obtain

$$g_t = \frac{1}{\alpha}\Big(f_t - \frac{\kappa}{\alpha+\kappa} \mathscr{P}_{\alpha\sigma}[f_t]\Big).$$

This equation together with (63) defines the explicit system for (33), (34). The linearization $z_t = Bz_{t-1}$ of this system at any equilibrium point with $s_* \in (-\sigma, \sigma)$ has the matrix

$$B = \frac{1}{1 - b_1 - ab_2} \begin{pmatrix} 1 - b_1 & a(1 - b_1) \\ b_2 & 1 - b_1 \end{pmatrix}.$$

Since

$$\det B = \frac{1 - b_1}{1 - b_1 - ab_2} > 1,$$

all these equilibrium states are unstable.

References

[1] *S. P. Anderson, A. de Palma, J.-F. Thisse*: Discrete choice theory of product differentiation. J. Econ. Literature *31* (1993), 1972.

[2] *G. Antinolfi, C. Azariadis, J. B. Bullard*: Monetary policy as equilibrium selection. Review, Federal Reserve Bank of St. Louis *89* (2007), 331–342.

[3] *M. Arnold, N. Begun, P. Gurevich, E. Kwame, H. Lamba, D. Rachinskii*: Dynamics of discrete time systems with a hysteresis stop operator. SIAM J. Appl. Dyn. Syst. *16* (2017), 91–119. zbl MR doi

[4] *J. Benhabib, R. E. A. Farmer*: Indeterminacy and sunspots in macroeconomics. Handbook Macroeconomics *1* (1999), 387–448. doi

[5] *A. Bick*: Threshold effects of inflation on economic growth in developing countries. Econ. Lett. *108* (2010), 126–129. doi

[6] *W. A. Branch*: Sticky information and model uncertainty in survey data on inflation expectations. J. Econ. Dyn. Control *31* (2007), 245–276. zbl doi

[7] *W. A. Brock, C. H. Hommes*: A rational route to randomness. Econometrica *65* (1997), 1059–1095. zbl MR doi

[8] *G. A. Calvo*: Staggered prices in a utility-maximizing framework. J. Monetary Econ. *12* (1983), 383–398. doi

[9] *C. D. Carroll*: Macroeconomic expectations of households and professional forecasters. Q. J. Econ. *118* (2003), 269–298. zbl doi

[10] *D. Colander, P. Howitt, A. Kirman, A. Leijonhufvud, P. Mehrling*: Beyond DSGE models: Toward an empirically based macroeconomics. Am. Econ. Rev. *98* (2008), 236–240. doi

[11] *R. Curtin*: Inflation expectations and empirical tests: Theoretical models and empirical tests. Inflation Expectations. Routledge International Studies in Money and Banking 56. Taylor & Francis, London, 2010, pp. 34–61.

[12] *P. De Grauwe*: Booms and busts in economic activity: A behavioral explanation. J. Econ. Behavior Organization *83* (2012), 484–501. doi

[13] *G. W. Evans, B. McGough*: Observability and Equilibrium Selection. University of Oregon, Eugene, 2015.

[14] *J. M. Frimpong, E. F. Oteng-Abayie*: When is inflation harmful? Estimating the threshold effect for Ghana. Am. J. Econ. Business Administration *2* (2010), 232–239. doi

[15] *M. Göcke*: Various concepts of hysteresis applied in economics. J. Econ. Surveys *16* (2002), 167–188. doi

[16] *M. Göcke, L. Werner*: Play hysteresis in supply or in demand as part of a market model. Metroeconomica *66* (2015), 339–374. zbl doi

[17] *A. Y. Ishlinskii*: Some applications of statistical methods to describing deformations of bodies. Izv. AN SSSR, Techn. Ser. *9* (1944), 580–590.

[18] *D. Kahneman, A. Tversky*: Prospect theory: An analysis of decisions under risk. Econometrica *47* (1979), 263–291. zbl MR doi
[19] *N. Kaldor*: The irrelevance of equilibrium economics. Econ. J. *82* (1972), 1237–1255. doi
[20] *M. S. Khan, A. S. Senhadji*: Threshold effects in the relationship between inflation and growth. IMF Staff Papers *48* (2001), 1–21.
[21] *M. A. Krasnosel'skii, A. V. Pokrovskii*: Systems with Hysteresis. Springer, Berlin, 1989. zbl MR doi
[22] *P. Krejčí*: Hysteresis and periodic solutions of semilinear and quasilinear wave equations. Math. Z. *193* (1986), 247–264. zbl MR doi
[23] *P. Krejčí, H. Lamba, S. Melnik, D. Rachinskii*: Analytical solutions for a class of network dynamics with mechanical and financial applications. Phys. Rev. E *90* (2014), Article ID 032822, 12 pages. doi
[24] *P. Krejčí, H. Lamba, S. Melnik, D. Rachinskii*: Kurzweil integral representation of interacting Prandtl-Ishlinskii operators. Discrete Contin. Dyn. Syst., Ser. B *20* (2015), 2949–2965. zbl MR doi
[25] *P. Krejčí, H. Lamba, G. A. Monteiro, D. Rachinskii*: The Kurzweil integral in financial market modeling. Math. Bohem. *141* (2016), 261–286. zbl MR doi
[26] *S. Kremer, A. Bick, D. Nautz*: Inflation and growth: New evidence from a dynamic panel threshold analysis. Empir. Econ. *44* (2013), 861–878. doi
[27] *H. Lamba, P. Krejčí, D. Rachinskii*: The global stability of a class of history-dependent macroeconomic models. Math. Model. Nat. Phenom. *15* (2020), Article ID 49, 24 pages. zbl MR doi
[28] *N. G. Mankiw, R. Reis*: Sticky information versus sticky prices: A proposal to replace the New Keynesian Phillips curve. Q. J. Econ. *117* (2002), 1295–1328. zbl doi
[29] *N. G. Mankiw, R. Reis, J. Wolfers*: Disagreement about inflation expectations. NBER Macroecon. Annual *18* (2003), 209–248. doi
[30] *J. F. Muth*: Rational expectations and the theory of price movements. Econometrica *29* (1961), 315–335. doi
[31] *L. Prandtl*: Ein Gedankenmodell zur kinetischen Theorie der festen Körper. Z. Angew. Math. Mech. *8* (1928), 85–106. (In German.) zbl doi
[32] *J. Robinson*: History versus equilibrium. Indian Econ. J. *21* (1974), 202.
[33] *J. Rudd, K. Whelan*: Can rational expectations sticky-price models explain inflation dynamics? Am. Econ. Rev. *96* (2006), 303–320. doi
[34] *M. Setterfield*: Should economists dispense with the notion of equilibrium? J. Post Keynesian Econ. *20* (1997), 47–76. doi
[35] *T. Vinayagathasan*: Inflation and economic growth: A dynamic panel threshold analysis for Asian economies. J. Asian Econ. *26* (2013), 31–41. doi

Authors' addresses: *Pavel Krejčí*, Faculty of Civil Engineering, Czech Technical University, Thákurova 7, 166 29 Praha 6, Czech Republic, e-mail: `Pavel.Krejci@cvut.cz`; *Eyram Kwame*, Regional Maritime University, P.O.BOX GP1115 Nungua, Accra-Ghana, West Africa, e-mail: `kwame@rmu.edu.gh`; *Harbir Lamba*, Department of Mathematical Sciences, George Mason University, 4400 University Dr, Fairfax, VA 22030, USA, e-mail: `hlamba@gmu.edu`; *Dmitrii Rachinskii* (corresponding author), *Andrei Zagvozdkin*, Department of Mathematical Sciences, University of Texas at Dallas, 800 W. Campbell Road, Richardson, Texas 75080-3021, USA, e-mail: `Dmitry.Rachinskiy@utdallas.edu`, `axz190001@utdallas.edu`.